NEW ZEALAND ACCELERATION RESPONSE SPECTRUM ATTENUATION RELATIONS FOR CRUSTAL AND SUBDUCTION ZONE EARTHQUAKES

Graeme H. McVerry[1], John X. Zhao[1], Norman A. Abrahamson[2] & Paul G. Somerville[3]

ABSTRACT

Attenuation relations are presented for peak ground accelerations (pga) and 5% damped acceleration response spectra in New Zealand earthquakes. Expressions are given for both the larger and the geometric mean of two randomly-oriented but orthogonal horizontal components of motion. The relations take account of the different tectonic types of earthquakes in New Zealand, i.e., crustal, subduction interface and dipping slab, and of the different source mechanisms for crustal earthquakes. They also model the faster attenuation of high-frequency earthquake ground motions in the volcanic region than elsewhere. Both the crustal and subduction zone attenuation expressions have been obtained by modifying overseas models for each of these tectonic environments to better match New Zealand data, and to cover site classes that relate directly to those used for seismic design in New Zealand codes.

The study used all available data from the New Zealand strong-motion earthquake accelerograph network up to the end of 1995 that satisfied various selection criteria, supplemented by selected data from digital seismographs. The seismographs provided additional records from rock sites, and of motions involving propagation paths through the volcanic region, classes of data that are sparse in records produced by the accelerograph network. The New Zealand strong-motion dataset lacks records in the near-source region, with only one record from a distance of less than 10 km from the source, and at magnitudes greater than M_W 7.23. The New Zealand data used in the regression analyses ranged in source distance from 6 km to 400 km (the selected cutoff) and in moment magnitude from 5.08 to 7.23 for pga, with the maximum magnitude reducing to 7.09 for response spectra data. The required near-source constraint has been obtained by supplementing the New Zealand dataset with overseas peak ground acceleration data (but not response spectra) recorded at distances less than 10 km from the source. Further near-source constraints were obtained from the overseas attenuation models, in terms of relationships that had to be maintained between various coefficients that control the estimated motions at short distances. Other coefficients were fitted from regression analyses to better match the New Zealand data.

The need for different treatment of crustal and subduction zone earthquakes is most apparent when the

[1] *Institute of Geological and Nuclear Sciences, Lower Hutt, New Zealand*
email: g.mcverry@gns.cri.nz

[2] *Pacific Gas and Electric Company, San Francisco, California, USA*

[3] *URS, Pasadena, California, USA*

effects of source mechanism are taken into account. For crustal earthquakes, reverse mechanism events produce the strongest motions, followed by strike-slip and normal events. For subduction zone events, the reverse mechanism interface events have the lowest motions, at least in the period range up to about 1s, while the slab events, usually with normal mechanisms, are generally strongest.

The attenuation relations presented in this paper have been used in many hazard studies in New Zealand over the last five years. In particular, they have been used in the derivation of the elastic site spectra in the new Standard for earthquake loads in New Zealand, NZS1170.5:2004.

1. INTRODUCTION

Response spectrum attenuation relations relevant to New Zealand have been required for the development of a new Standard for earthquake loads in New Zealand, NZS1170.5:2004 (Standards New Zealand, 2004), for seismic hazard assessments for the construction or strengthening of several major buildings and bridges, and for design reviews and strengthening of hydro-electricity dams. Of relevance to the Standard is that Wellington and some other cities are located close to major active faults that have estimated recurrence intervals of a few hundred years for earthquakes causing surface-fault rupture, while the hazard analysis (Matuschka *et al.*, 1985) on which the seismic coefficients of the previous New Zealand Loadings Standard NZS4203:1992 (Standards New Zealand, 1992) were based did not account for near-fault motions. Many dams are located near faults that are less active, with recurrence intervals of several thousand years, but which are still critical for the 10,000 year return period motions that are often considered as the Maximum Considered Earthquake motions in the design or assessment of these structures.

Development of appropriate response spectrum attenuation relations is complicated by the tectonic setting in New Zealand, with both shallow crustal earthquakes and those associated with two subduction zones being important. New Zealand is located across the boundary of the Pacific and Australian plates, with the nature of the plate boundary changing through the country (Figure 1). To the north-east, in the Hikurangi subduction zone, the Pacific Plate subducts beneath the Australian Plate under the North Island. The plate boundary interface lies beneath Wellington and other cities, at depths of 20 to 30 km. In Fiordland in the southwest of the South Island, the sense of subduction is reversed, with the Pacific Plate overlying the Australian Plate. The two subduction zones are linked by a region of oblique convergence, dominated by the Alpine Fault but also including other major predominantly strike-slip faults with some reverse movement in the Axial Tectonic Belt. The Taupo Volcanic Zone is an extensional zone, with shallow normal-faulting earthquakes. It is also a region of high attenuation, both in the shallow crust and in the underlying mantle. Normal mechanisms also prevail in the western and northern North Island. There are also zones of predominantly reverse faulting, in the north-western and south-eastern South Island. This tectonic setting leads to a mix of different types of earthquakes to be considered in developing attenuation models: strike-slip, oblique, reverse and normal mechanism crustal earthquakes, and subduction zone earthquakes associated both with the subduction interface and within the downgoing slabs. Both subduction zone and crustal earthquake motions, including near-source motions from large-magnitude earthquakes, must be considered in the seismic design for major centres and important infrastructure facilities.

In New Zealand, like many regions of the world, there were until recently insufficient recordings of strong earthquake motions to develop attenuation relations from local data. However, after more than forty years of operation of a strong-motion accelerograph network, which has grown gradually since its initial deployment in 1963 (e.g. Cousins, 1993), and especially because of the occurrence of several magnitude 6 to 7 earthquakes over the period 1984 to 1995, it has now become possible to develop attenuation relations appropriate for New Zealand.

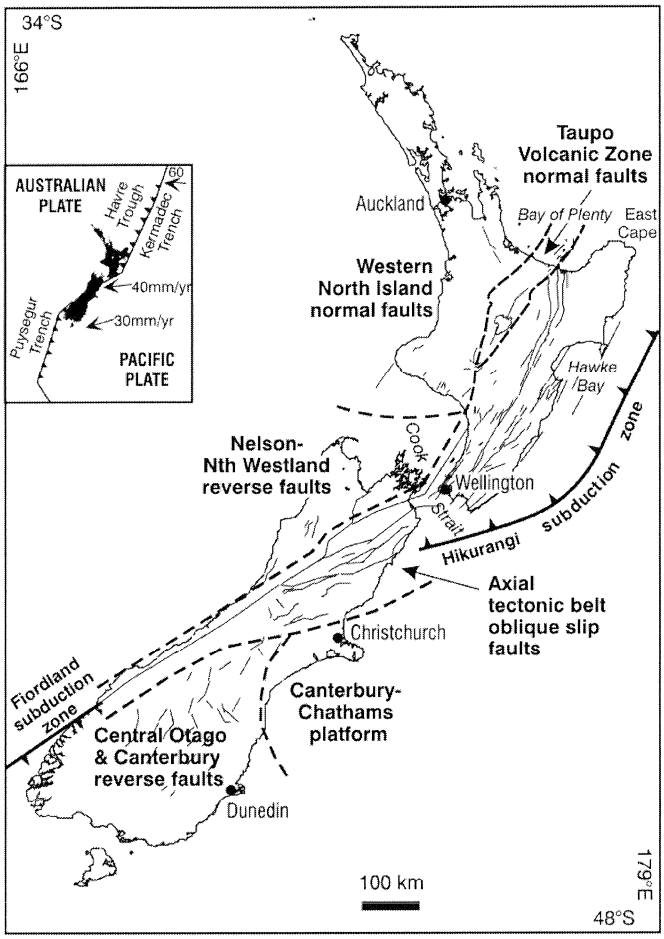

Figure 1: The plate tectonic setting of New Zealand, with the Pacific plate subducting under the Australian plate in the Hikurangi subduction zone to the north-east, and the Australian plate subducting under the Pacific plate in the Fiordland subduction zone in the southwest. The Taupo Volcanic Zone is an extension zone characterised by normal faulting and high attenuation. The predominant faulting mechanism regimes in other regions are also shown.

1.1 Previous New Zealand attenuation studies

The New Zealand Loadings Standard NZS4203:1992 was based on a seismic hazard analysis by Matuschka *et al.* (1985), which used the Katayama (1982) response spectrum relation from Japan, modified to better match the few New Zealand response spectra available at the time (Mulholland 1982; 1983; Berrill, 1985; McVerry, 1986). With the additional strong-motion data that became available between 1984 and 1995, it was possible and timely to develop an attenuation model for acceleration response spectra based largely on New Zealand data to use in the seismic hazard studies for a new Standard, published recently as NZS1170.5:2004.

There have been several attenuation studies making use of a similar dataset of New Zealand earthquake ground-motion records as used in the current study, sometimes as in this study supplemented by overseas near-source data. Zhao *et al.* (1997) found that New Zealand pgas depend strongly on source depth. Interaction with the current response spectrum study led to a distinction between different tectonic categories of earthquakes in the peak ground acceleration relations. Cousins *et al.* (1999) considered the effects of weak versus strong rock, and volcanic path attenuation, using

a mixture of accelerograph and seismograph records from mainly rock sites. The study of volcanic path effects included the use of records obtained during a temporary deployment of seismographs for other purposes in the Taupo Volcanic Zone, with this temporary deployment including some instruments at soil sites. The Cousins *et al.* model did not include magnitude saturation effects at short distances, and gives unrealistically high pga estimates at short distances for large magnitude earthquakes, especially for strong rock sites (see for example the plots for magnitude 8 in their Figure 14). Dowrick & Rhoades (1999) developed attenuation models for Modified Mercalli intensity for shallow and deep earthquakes that included a depth term and included increased attenuation for the volcanic zone, updating earlier studies that lacked these features.

1.2 Scope of the current study

The work described in the current paper presents in detail for the first time in an openly available publication the response spectrum attenuation model that was used in the development of the Hazard Factor maps and spectra of the recently published Standard NZS1170.5. This paper considerably extends the presentation given previously at the 12th World Conference of Earthquake Engineering (McVerry *et al.*, 2000). The model has also been used by the Institute of Geological and Nuclear Sciences (GNS) in many seismic hazard studies in New Zealand over the last five years, including GNS's National Seismic Hazard Model (NSHM) (Stirling, 2000; Stirling *et al.*, 2000; 2002).

The attenuation model was developed in stages between 1997 and 2001 in collaborative studies between the New Zealand and US authors of this paper. The US authors presented an initial model, which was developed in close collaboration with the GNS staff, in a client report in 1997, referred to in this paper as the WCFS report. Further developments have occurred at GNS in consultation with the US authors, using the random effects methodology and software of Abrahamson and Youngs (1992), as provided by Norm Abrahamson. The initial use of the model was in several seismic hazard studies of major infrastructure facilities in New Zealand. During these studies, the model was subjected to intensive international review, with the review recommendations incorporated in later versions of the model.

The paper presents a model for estimating the strength of earthquake ground motions that is consistent with New Zealand data; recognises the various tectonic types of earthquakes in New Zealand; supplements New Zealand data with overseas peak ground acceleration (pga) records for the magnitude and distance ranges (i.e. near-source or large-magnitude) that are lacking in the local data; and constrains near-source behaviour by overseas attenuation relations.

2. TECTONIC CATEGORIES AND EARTHQUAKE SOURCE MECHANISMS

2.1 Tectonic Source Categories

An important aspect of this study is that it recognises the various tectonic types of earthquakes in New Zealand, rather than mixing subduction zone and crustal earthquakes. As noted in the review by Abrahamson & Shedlock (1997), various studies (e.g. Youngs *et al.*, 1997; Atkinson & Boore, 2003) show that earthquake motions from subduction earthquakes generally attenuate less rapidly than those from crustal earthquakes in plate margin regions. Mixing the two types of earthquakes will not only over-predict one type and under-predict the other, but may also cause difficulties in the regression analyses because of the combination of different attenuation behaviour. The subduction zone earthquakes have been further subdivided, with three tectonic source categories included in the final model: crustal, plate interface and slab. Slab earthquakes generally produce stronger motions than interface earthquakes of the same magnitude and distance, with the strength of motion for a given magnitude and distance increasing with source depth (e.g. Youngs *et al.*, 1997; Kobayashi *et al.*, 2000). These subdivisions are in line with modern practice (e.g. Abrahamson & Shedlock, 1997; Somerville, 2000; Atkinson & Boore, 2003).

The tectonic source categories are explained with reference

to the tectonic setting of New Zealand, summarised in Figure 1. New Zealand has three distinct categories of earthquakes, illustrated by seismicity across the Hikurangi margin in the southern part of the North Island in the cross-section view in Figure 2. The earthquake source and ground-motion characteristics of these categories of earthquakes (crustal, interface and slab) are expected to be different, based on worldwide data. The first category of earthquakes consists of earthquakes occurring in the shallow crust of the overlying plate, in this case the Australian plate. The remaining categories covering subduction zone earthquakes can be distinguished from crustal earthquakes by their location and depth. The second category consists of earthquakes occurring on the interface between the Pacific and Australian plates. These have predominantly reverse mechanisms with some strike-slip, are at depths of less than 50 km (Youngs *et al.*, 1997; Atkinson & Boore, 2003), although at a maximum depth of 24 km in the New Zealand database used in this study, and are distinguished by their location in 3-D space at the plate interface. The third category consists of earthquakes occurring in the slab source zone within the subducted Pacific plate, with the predominant mechanism of the slab earthquakes changing with depth.

Seismicity cross-sections, such as that shown in Figure 2, are not sufficient to distinguish between interface and slab events, with the discrimination between these events depending largely on source mechanism.

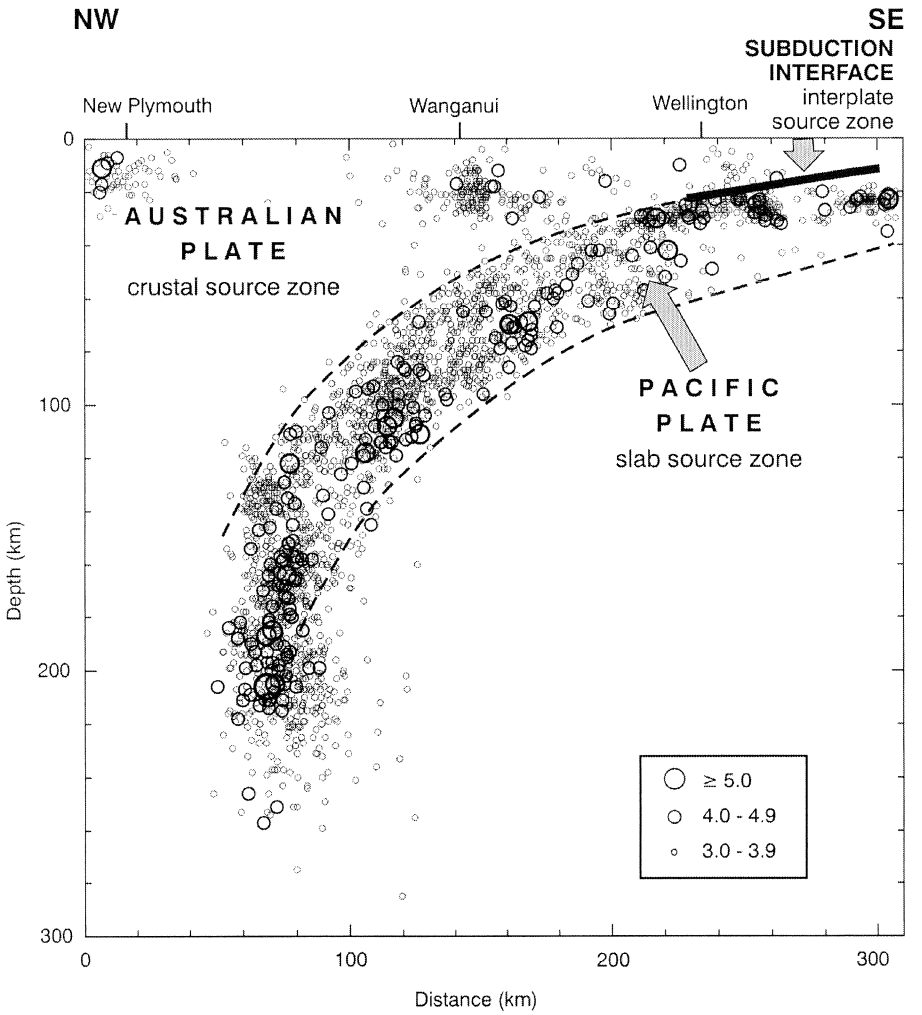

Figure 2: Cross-section of seismicity in the Hikurangi margin demonstrating different tectonic source categories of earthquakes.

The shallower slab earthquakes, to depths of about 40 km, are associated with an extensional regime as the downgoing slab bends under its own weight, so have predominantly normal or oblique focal mechanisms, with one event in our dataset having a strike-slip mechanism. All normal-mechanism subduction zone earthquakes are shallow slab events. The shallow slab earthquakes in our dataset occurred beneath the southeast coast of the North Island at depths of 41 km or less. The normal mechanisms of the shallow slab events contrast with the reverse thrust events at shallow depths marking the subduction interface. A compressional regime gives rise to reverse or strike-slip focal mechanisms at greater depth in the slab, but these events are clearly separated from interface events by their greater depths. The deep slab earthquakes in our dataset mainly occur beneath the central part of the North Island at depths of 60 km or more.

We chose the rupture centroid depth of 50 km to separate these two sets of slab events. The exact choice of the depth separating the shallow and deep slab events turned out to be unimportant for our dataset, in which there were no data satisfying the selection criteria (see Section 3.2) from earthquakes between depths of 40 and 60 km, although the density of earthquakes in this depth range shown in Figure 2 suggests that the separation depth could become more of an issue as the New Zealand strong-motion dataset becomes larger. Also, despite their different mechanisms, it was found that there was no statistically significant difference between the spectra of shallow and deep slab earthquakes that could not be accounted for by a simple depth term (see Section 7).

In addition, there are further complications in the region of volcanism and extension in the Taupo Volcanic Zone (TVZ), as illustrated schematically in Figure 3a. In general, geometrical spreading provides most of the reduction in ground motions for the travel distances up to 100-200 km which are usually of interest for strong-motion attenuation relations. However, there is also energy loss from dissipative mechanisms in the medium, referred to as anelastic attenuation, that gives rise to an additional exponential decay $e^{-\pi rf/Q(f)\beta}$ of wave amplitude with travel distance r, frequency f, wave velocity β, and the quality factor $Q(f)$. The anelastic attenuation rate is characterised by the inverse of the quality factor, with high attenuation rates corresponding to low Q. The subducting slab of the Pacific Plate has very low attenuation, the crust of the Australian Plate has moderate attenuation, and the mantle wedge between the slab and the overlying crust has very high attenuation. The crust in the TVZ also has very high attenuation. This variation of attenuation is shown in the Q-inversions of Eberhart-Phillips and Chadwick (2002). In regions of low Q, anelastic attenuation can be as important as geometric attenuation even for path lengths of only a few tens of kilometres. The difference in attenuation rates along the various paths is manifested by intensity patterns for deep slab earthquakes in the Hikurangi subduction zone being displaced to the east from the epicentre, as demonstrated in Figure 3b by the isoseismal map of the 5 January 1973 earthquake (Downes, 1995), for example. Thus deep earthquakes in the subducting slab under the TVZ are felt more strongly to the east in the Hawkes Bay, at locations involving low-loss slab paths, than at shorter distances above the source region, at locations involving paths through the mantle wedge and TVZ crust.

Only data involving low-loss slab paths are included in the modelling used to derive the attenuation expressions for deep slab earthquakes in this paper. Consequently, the model is not appropriate for source-to-site combinations where the propagation path is through the highly attenuating mantle wedge, for example from deep slab sources to Taupo and Rotorua in the volcanic region and extending north westwards along the Waikato River valley. Eberhart-Phillips and McVerry (2003) provide attenuation expressions for the high-loss mantle paths, through location-dependent modification terms to the model presented in this paper. The model presented here does account for high-loss crustal paths in the TVZ for crustal, interface or shallow slab earthquakes, through an additional term for volcanic path attenuation (see Section 9.1).

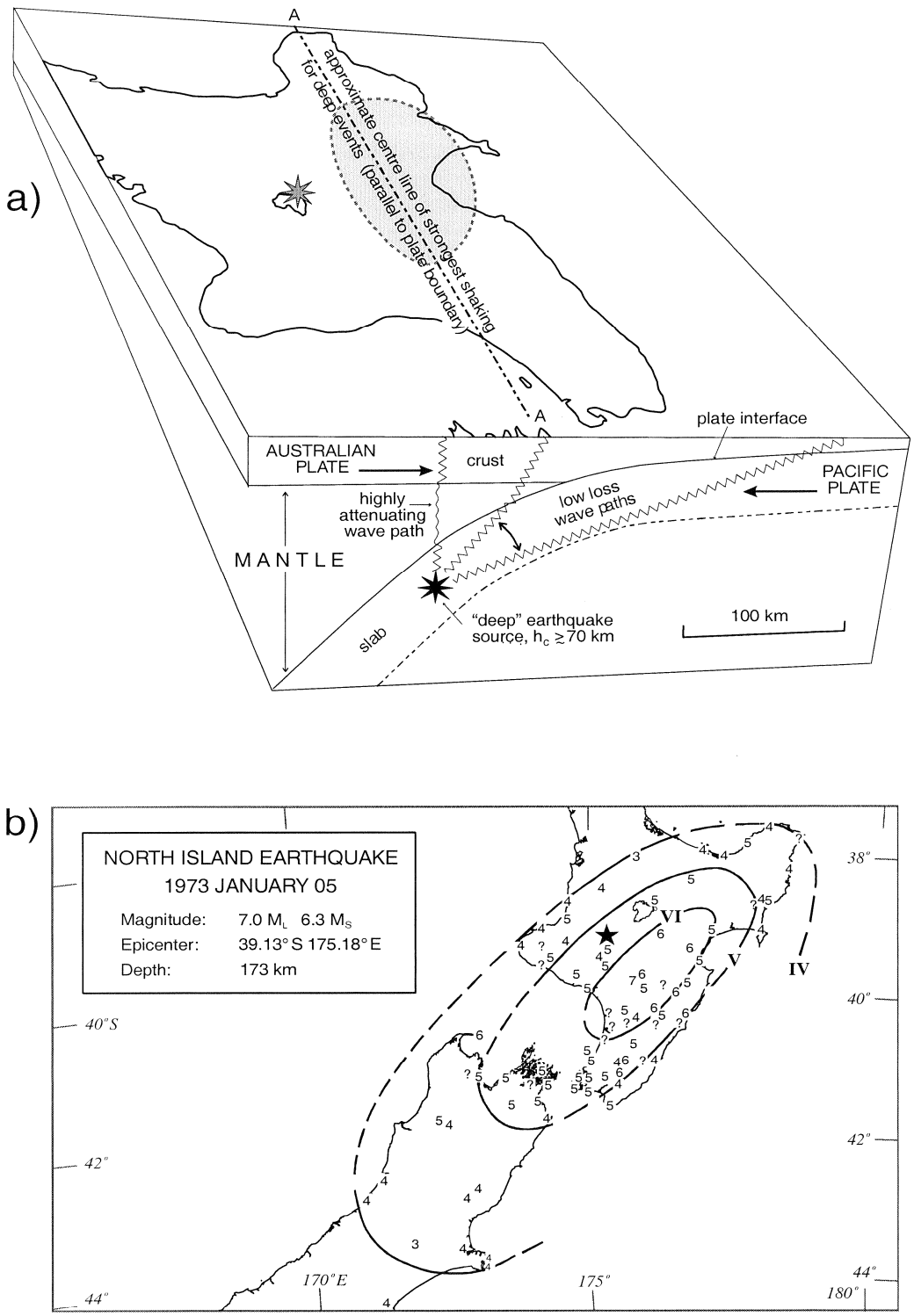

Figure 3: (a) Schematic view comparing low-loss paths up the subducting slab and highly-attenuating paths through the mantle and crust under the Taupo Volcanic Zone. The attenuation expressions presented in this paper for deep slab earthquakes apply only for low-loss paths up the slab (after Dowrick & Rhoades, 1999). (b) An example of the isoseismal pattern of a deep slab earthquake being offset to the east of its epicentre, marked by a star (Downes, 1995).

2.2 Earthquake Source Mechanisms

Source mechanism was found to be an important parameter in characterising earthquake spectra in this study. For crustal earthquakes, dependence on four source-mechanism categories (strike-slip, normal, oblique-reverse, and reverse) is included in the attenuation expressions through source-mechanism terms. For subduction zone earthquakes, the mechanism is one of the factors used in determining tectonic type, but was found to be not a significant extra parameter in addition to tectonic type in the attenuation expression.

Source-mechanism on its own without tectonic type is not sufficient to characterise ground-motion effects. For example, peak ground accelerations tend to be greater for crustal reverse-mechanism earthquakes than for crustal strike-slip or normal-mechanism earthquakes, but thrust earthquakes on the subduction interface, which have a reverse mechanism, tend to produce lower pgas than shallow subduction-slab earthquakes with normal mechanisms. These effects have been demonstrated previously for New Zealand pgas in the study by Zhao *et al.* (1997).

The focal mechanism categories are based on the rake angle, which is the angle in the fault plane between the strike of the fault (the azimuthal direction of a horizontal line on the fault plane) and the direction of slip of the hanging wall. Pure strike-slip faults have rakes of 0° or ±180°, a pure reverse fault has a rake of 90° and a pure normal fault a rake of -90°. The definitions adopted for the focal mechanism categories in this study are: strike-slip having rake angles between 0 and 33 degrees, 0 and –33 degrees, 147 and 180 degrees, and –147 and –180 degrees; normal having rake angles between –34 and –146 degrees, oblique (with a reverse component) having rake between 33 and 66(56?) degrees and between 124 and 146 degrees, and reverse having rake between 67(57?) and 123.

The New Zealand earthquakes providing data that were used in this study are listed in Table 1 (adapted from Zhao *et al.*, 1997).The table includes the tectonic category and source mechanism for each earthquake, together with its event time and location.

TABLE 1: NEW ZEALAND EARTHQUAKES CONSIDERED IN THIS STUDY
(Adapted from Zhao *et al.*, 1997)

No.	yr	Date mo	dy	UT hr/min	Epicentre °S	°E	M_w	Centroid depth H_C (km)	Tect. Type	Predom Mech. /Region
1*	1966	03	04	2358	38.45	177.91	5.64	24	I	R
2	1966	04	23	0649	41.63	174.40	5.75	19	C	O
3∇	1968	05	23	1724	41.76	171.96	7.23	10	C	R
4	1968	09	25	0702	46.49	166.68	6.27	4	C	S
5	1971	08	13	1442	42.13	172.10	5.70	9	C	S
6	1972	01	08	2133	37.57	175.69	5.27†	7	C	N
7	1973	01	05	1354	39.04	175.25	6.57	149	S	R
8	1974	11	05	1038	39.65	173.63	5.44	17	C	N
9	1975	06	10	1011	40.34	175.93	5.62	38	S	N
10	1976	05	04	1356	44.67	167.45	6.51	10	C	O
11	1977	01	18	0541	41.73	174.30	6.02	34	S	N
12	1977	05	11	0241	43.26	171.73	5.20	10	C	S
13	1979	03	24	2106	41.94	171.63	5.08	10	C	R
14	1980	06	23	1645	39.90	175.60	5.49	61	S	R
15	1980	10	05	1532	39.70	176.82	5.66	36	S	N
16*	1980	11	25	0457	37.78	178.97	5.54	41	S	N
17	1982	02	05	1751	40.64	175.92	5.36	34	S	N
18	1982	09	02	1558	39.74	176.93	5.46	31	S	N
19	1984	03	05	0207	38.92	175.78	5.27†	9	C	NV[(1)]
20	1984	03	08	0040	38.31	177.29	5.91	80	S	R
21	1984	06	24	1329	43.60	170.56	6.14	13	C	S
22	1985	07	19	1433	38.72	177.30	5.92	31	S	N
23∇	1987	03	02	0142	37.88	176.84	6.53	6	C	N
24	1988	06	03	2327	45.10	167.17	6.69	60	S	R
25	1989	05	31	0554	45.27	166.88	6.33	24	I	SR
26	1989	08	08	0759	40.12	174.30	5.40	112	S	R
27∇	1990	02	10	0327	42.32	172.74	5.93	8	C	S
28∇	1990	02	19	0534	40.38	176.22	6.23	27	S	N
29∇	1990	05	13	0423	40.35	176.23	6.37	13	C	R
30	1990	08	15	1554	40.32	176.44	5.17	28	S	N
31	1990	10	04	2348	41.60	175.41	5.57	15	I	R
32	1990	10	06	0241	41.60	175.41	5.46	15	I	R
33	1991	01	28	1258	41.89	171.58	5.79	10	C	R
34	1991	01	28	1800	41.90	171.67	5.93	11	C	R
35	1991	02	15	1048	42.04	171.59	5.42	9	C	R
36	1991	07	12	0442	39.31	175.97	5.30	69	S	S
37	1991	09	08	1350	40.25	175.17	5.61	94	S	R
38	1992	03	02	0905	40.31	176.48	5.54	26	S	N
39	1992	03	30	0702	43.05	171.23	5.50	5	C	R
40	1992	05	16	1757	38.23	178.37	5.76	22	I	R
41	1992	05	27	2230	41.63	173.62	5.88	67	S	S
42	1992	06	21	1743	37.67	176.86	6.25	4	C	NV
43∇	1993	04	11	0659	39.74	176.52	5.63	24	I	R
44∇	1993	08	10	0051	45.21	166.71	6.81	22	I	R
45∇	1993	08	10	0946	38.52	177.87	6.19	39	S	S
46∇	1994	06	18	0325	43.01	171.46	6.81	4	C	R
47	1994	12	15	1120	37.27	177.53	6.31	12	C	SV
48	1995	02	05	2251	37.65	179.49	7.09	10	C	N
49	1995	02	10	0145	37.92	179.51	6.49	10	C	N
50	1995	03	22	1943	41.05	174.18	5.83	90	S	S
51∇	1995	11	24	0619	42.98	171.8	6.24	5	C	O

Notes for Table 1

∇ Distances measured from nearest part of source (rupture surface)
† M_w inferred from M_s
* No data from this event satisfied selection criteria for regression analyses

(1) V = Event with travel paths in the Central Volcanic Region
Tectonic type: C = Crustal, I = Interface, S = Slab
$H_C \leq 50$ km for shallow slab earthquakes, $H_C > 50$ km for deep slab earthquakes
Source mechanism: N = Normal, R = Reverse, O = Oblique (predominantly reverse) SR = predominantly strike-slip with reverse component S = Strikc-slip
See Zhao *et al.* (1997) for references for source properties.

3. PEAK GROUND ACCELERATION AND RESPONSE SPECTRUM DATASETS

3.1 New Zealand Earthquake Ground Acceleration Data

The New Zealand dataset as used for the Zhao *et al.* (1997) peak ground acceleration (pga) attenuation model served as the starting point for the response spectrum acceleration (SA) model. However, for periods other than 0s, corresponding to pga, there were fewer records from this dataset available for the modelling, because acceleroscope records and undigitised film records contribute pgas but not spectra and because of more restrictive selection criteria for the spectra (see Section 3.2). The SA study used records from 49 New Zealand earthquakes between 1966 and 1995 (Table 1), two fewer than in the pga study because two earthquakes (event numbers 1 and 16) had no records that satisfied the SA selection criteria.

The pga and response spectrum attenuation data consist of values for two orthogonal horizontal components, generally aligned along the instrument axes for mechanical-optical or digital accelerographs, and for the NS and EW components for scratch-plate pga records. Pgas from undigitised film records are aligned at 45 degrees to the instrument axes, corresponding to the directions in which they were recorded by the New Zealand mechanical-optical accelerographs, with standard processing rotating the components to be aligned with the instrument axes. Attenuation expressions are presented later for both the stronger and the geometric mean of the two horizontal components. Note that the stronger component corresponds only occasionally with the strongest resolved horizontal component, for which the direction in general varies with spectral period.

The breakdown of New Zealand events by tectonic class and mechanism is summarised in Table 2, together with the magnitude range for each category. The balance of crustal and subduction zone earthquakes is almost even, with 24 crustal and 25 subduction zone events providing data that were used in the analysis.

TABLE 2: DISTRIBUTION OF NEW ZEALAND EARTHQUAKES BY TECTONIC CLASS AND MECHANISM

Tectonic Class	Mechanism	Magnitude Range	ΔM
24 Crustal	8 Reverse	5.08-7.23	2.15
	3 Reverse-oblique	5.75-6.52	0.76
	6 Strike-slip	5.20-6.31	1.11
	7 Normal	5.27-7.09	1.82
Subduction Zone			
6 Interface (plus one reverse with Site Class E data only)	5 Reverse	5.46-6.81	1.35
	1 Strike-slip with reverse component		
10 Shallow slab (plus one with Site Class E data only)	9 Normal	5.17-6.23	1.06
	1 Strike-slip		
9 Deep slab	6 Reverse	5.30-6.69	1.39
	3 Strike-slip		

The distribution of the data is shown as functions of centroid depth and moment magnitude in Figure 4(a), and of moment magnitude and source distance in Figure 4(b), with symbols indicating the earthquake type (tectonic class, together with

source mechanism for crustal earthquakes). Source distance is intended to represent the shortest distance from the site to the earthquake rupture surface, and is discussed in greater detail in Section 6. Open symbols indicate earthquakes or records with only pga data, while solid symbols indicate that there are response spectra data. The open symbols at distances less than 10 km for crustal earthquakes represent overseas pga data that have been used to supplement the New Zealand data at short distances (see Section 3.3), while those for magnitude M_w 7.23 represent the pga data from the Inangahua earthquake.

Overall, the magnitude range is somewhat limited, from M_w 5.08 to M_w 7.23. The range is very limited, to less than 1.2 magnitude units, for the crustal strike-slip, crustal reverse-oblique and shallow slab categories. The largest magnitude is for the 23 May 1968 Inangahua earthquake, but this earthquake produced only pga data from scratch-plate acceleroscopes, with no response spectra data. The largest magnitude New Zealand earthquake for which response spectra were available was the M_w 7.09 East Cape earthquake of 5 February 1995, but the closest of the records from this event was obtained at a distance of 169 km. The largest earthquake to produce a response spectrum within 20 km of the source was the M_w 6.81 Arthurs Pass earthquake of 18 June 1994. The largest magnitude for subduction zone events was also 6.81, for the Secretary Island earthquake of 10 August 1993 on the Fiordland subduction interface.

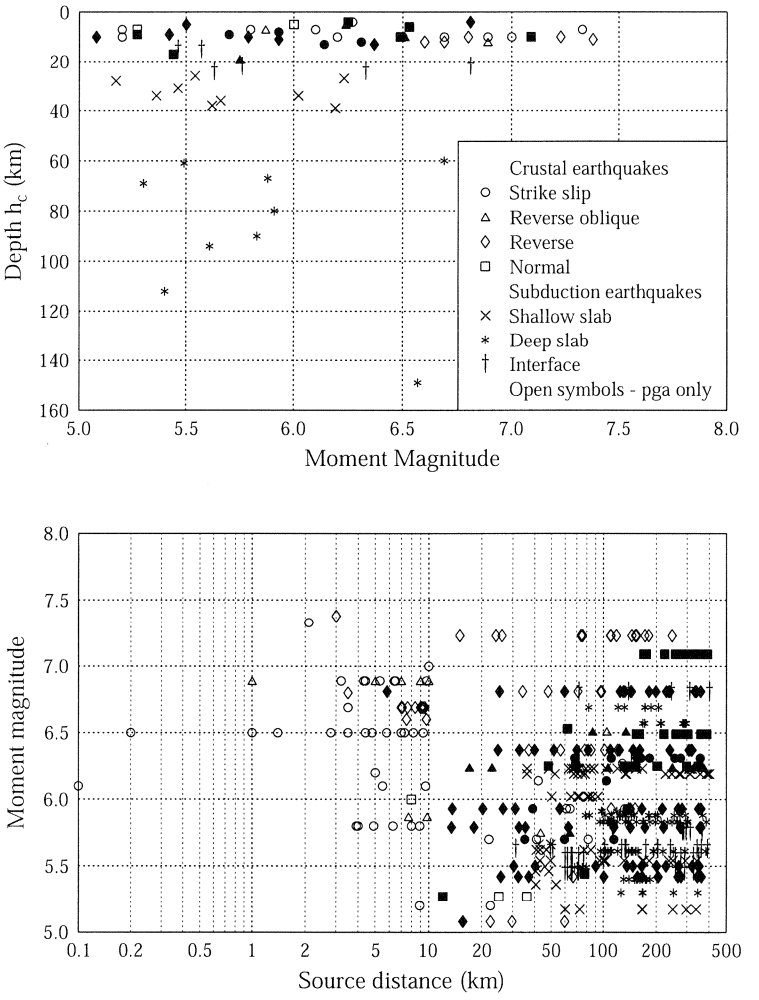

Figure 4: Distribution of data by (a) depth and magnitude; and (b) magnitude and distance. The symbols indicate the tectonic class of the earthquakes, and also source mechanism for crustal earthquakes. Open symbols are records for which only peak ground accelerations were used, while solid symbols represent response spectrum data. The pga records at distances less than 10 km represent overseas data used to supplement the New Zealand data (see Section 3.3).

Centroid depths range from 4 km to 149 km, with only 9 of the 49 events at depths greater than 50 km. The dataset excludes deep slab data involving travel paths through the highly attenuating mantle region under the central North Island.

The largest New Zealand horizontal peak ground acceleration is 0.58g recorded at Reefton in the 1968 Inangahua earthquake (M_w 7.23), 15 km from the modelled rupture surface, but this was provided by a scratch-plate acceleroscope instrument which does not provide acceleration histories from which spectra can be calculated. The strongest peak ground acceleration from a record providing response spectra was 0.44g from the Arthurs Pass Police Station at a distance of 6 km from the source in the magnitude 6.81 Arthurs Pass earthquake of 18 June 1994. This is the shortest source-to-site distance for New Zealand records, with the next closest 12 km. The shortest distance of the subduction zone records is 31 km. Horizontal distances used range up to 400 km.

3.2 Selection Criteria

An important selection criterion for the New Zealand records used in the attenuation studies was that they came from events for which moment magnitudes M_W are available, as correlations between M_L and M_W are poor for New Zealand earthquakes (Dowrick and Rhoades, 1998). Also, centroid depth, mechanism type, source-to-site distance and a description of site conditions were required.

The Te Aroha and Tokaanu earthquakes (event dates 1972 01 08 and 1984 03 05 in Table 1) were included even though they have no seismic moments available, because they are important for their locations just outside and within the Central Volcanic Region respectively. For these two events, moment magnitude M_W was estimated from surface-wave magnitude M_S, using the relationship of Dowrick & Rhoades (1998). These two events were used only for residual analyses in the Zhao *et al.* (1997) study, but were included in the regressions here.

Records included in the regressions were required to satisfy minimum pga criteria that depended on the resolution of the instrument on which the recording was made. The smallest values considered to be sufficiently accurate were:

- acceleroscopes (scratch-plates): 0.02g
- mechanical-optical accelerographs (i.e. film-recording): 0.01g
- digital 12-bit accelerographs: 0.004g
- digital 16-bit accelerographs : 0.0005g

The data were reviewed to find sites that might be subject to excessive amplifications for their site class. The only sites excluded for this reason were Atene A on the top of a steep conical hill (McVerry *et al.*, 1984), which exhibits strong topographical effects, and Hanmer Springs which exhibits a site resonance at 1.5-1.7 Hz.

Two selection criteria additional to those used for the Zhao *et al.* pga study were applied to be consistent with criteria used for the models of Abrahamson & Silva (1997) and Youngs *et al.* (1997), which served as the starting points for the crustal and subduction zone attenuation expressions developed in the current study.

First, all sites classified as class E (very soft soil sites with about 10 m or more of material with estimated shear-wave velocities of less than 150 m/s, see site classifications in Section 4) were excluded to be consistent with the Abrahamson & Silva and Youngs *et al.* studies (N.Abrahamson, pers. comm.), although this exclusion was not spelled out in either of these papers. This criterion excluded 40 SA records that would otherwise have been included, plus 7 pga-only records.These sites were excluded not because of the possibilities of large amplifications, but more because their spectra appear to have site-specific characteristics instead of fitting generic site-class shapes.

Second, records from the bases of buildings greater than four storeys in height were excluded, because of concerns that they may have been influenced by structural response. This eliminated a total of 33 records that would have been used otherwise, mainly from central Wellington.

Data from very deep events were restricted to those in which travel paths from source to site through solid slab or crustal rock were possible, i.e. travel paths passing through the highly attenuating mantle were excluded.

The combination of these criteria led to the reduction of the 461 New Zealand accelerograph records used in the pga study to 224 records in the response spectrum study at short-period. The response spectrum values have been used in the attenuation model regressions only for periods where they exceed the estimated noise levels of the combined recording and processing systems (Cousins *et al.*, 1999) i.e. up to the record-dependent period of the initiation of the high-pass filter roll-off used in the processing of the records to eliminate possible long-period noise. This signal-to-noise criterion further reduced the number of records used to model long-period spectral ordinates to only 166 records judged to be above noise-level at 2.0s. However, these records were supplemented by digital seismograph records (see Section 3.4), which increased the number of New Zealand pga records used in this study to 535 despite the more restrictive selection criteria, with 435 of these records providing response spectra. In addition, the data set was supplemented by 66 overseas near-source pga records (see Section 3.3).

3.3 Supplementary Overseas PGA Data

There is a lack of near-source records in the New Zealand response spectrum dataset. There are only 11 records at distances of less than 25 km from the source in crustal earthquakes, with 7 of these from 3 sites (3 from Te Kuha at the mouth of the Buller Gorge near Westport, and 2 each from Arthurs Pass and Flock Hill station in the 8 June 1994 Arthurs Pass and 24 November 1995 Cass earthquakes).

To constrain the model at short distances where New Zealand records are lacking, near-source overseas pga data consisting of 66 records from 17 crustal earthquakes with moment magnitudes ranging from 5.2 to 7.4 were included. These data were restricted to those from sites at distances of 10 km or less from the source, less than the distance of all but one record in the New Zealand dataset, with a shortest distance of 0.1 km. The other criteria for selecting the overseas data were consistent with those used for the New Zealand data. Thus a moment magnitude had to be available for the event, and its centroid depth, source mechanism and the shortest distance from site to source were also required. In addition, enough had to be known about each site for its ground class to be assigned on the same basis as for the New Zealand sites. The pgas of the selected overseas records ranged from 0.11g to 0.98g, with 18 of the 66 recordings having pgas stronger than the largest value (0.58g) in the New Zealand dataset. Many of the records that we used were contained in the compilation by Otsuka *et al.* (1993), which contained near-source data from Campbell (1981), although we often obtained supplementary information about required parameters from other sources, and also included records that were more recent than those compilations. The overseas data were not intended to be comprehensive for the 0-10 km distance range, but were felt to be representative, and included data from Northridge and Kobe.

It is possible that New Zealand earthquakes may produce peak accelerations at short distances that are different to those from earthquakes in some other parts of the world. However, it was felt preferable to use overseas data to provide some near-fault constraints rather than to have very high values that were unconstrained by data and were difficult to justify in terms of motions recorded anywhere in the world.

Only pgas rather than the full response spectra were used for the overseas records added to the dataset for this study, because response spectra for many of the records were not available at GNS when the near-source records were added in 1995. The response spectra for the overseas records have now been compiled at GNS, together with further records from recent earthquakes, and are now available to provide near-source data constraint at all spectral periods for future studies.

3.4 Seismograph Records for Volcanic Path Attenuation and Moderate-to-Strong Rock Sites

There are very few records available from the New Zealand

strong-motion accelerograph network from sites on moderate- to high-strength rock, in that most of the strong-motion accelerograph sites are on soil, with the few rock sites generally being on weak rock. Also, there are few records that have propagation paths through the volcanic region, partly because the attenuation in that region is apparently so rapid that the motions for paths that completely cross it are reduced to levels below those generally recorded by strong-motion instruments. There are very few accelerograph sites within the volcanic region to record motions from earthquakes within it. To obtain sufficient rock-site and volcanic-path data for the response spectrum study, records from digital seismographs installed as part of the New Zealand National Seismograph Network since 1990 were used to supplement the accelerograph data. Seismograph records from a temporary deployment in the volcanic region from January to May 1995 were used to further augment the data. Earlier studies (e.g. Cousins *et al.*, 1999) have established that acceleration records virtually identical to those recorded directly by accelerographs can be recovered from the seismograph records. As well as converting the seismograph records to acceleration records, the processing has included correcting the accelerograph and seismograph records for instrument response characteristics. The seismograph records have contributed significantly to the determination of volcanic path attenuation, as discussed in Section 9.1.

4. CLASSIFICATION OF SITE CONDITIONS

One of the main justifications for the development of response spectrum attenuation relations for New Zealand was to use them in a national seismic hazard study to underpin a revision of the loadings standard. It was therefore desired to retain site classifications as close as possible to those of the three subsoil categories (a)-(c) of the New Zealand Loadings Standard NZS4203:1992 (Standards New Zealand, 1992) that was current when the attenuation study was performed. Category (a) of that standard nominally corresponds to rock or very stiff soil sites with estimated natural periods less than 0.25s, category (b) corresponds to intermediate soil sites and category (c) corresponds to flexible or deep soil sites with natural periods greater than 0.6s.

Some minor modifications have been made to the NZS4203 site classes, based on statistical analyses that demonstrate significant differences between spectra from different site classes and similarity among those from sites within the same class, as described in the following.

The new site class definitions are listed in Table 3. They include depth boundaries between Class C Shallow Soil Sites and Class D, Deep or Soft Soil Sites, given in Table 4, which are unaltered from those between the NZS4203:1992 Intermediate and Flexible or Deep Soil Sites. The new classification has been adopted in the recently published standard NZS1170.5:2004.

The NZS4203 category (a) has been subdivided into: rock sites, or sites with soil layer of thickness not exceeding 3 metres overlying rock; and category (a) sites with soil layer of thickness greater than 3 metres (labelled aL, for "a layered", in this paper). Rock is taken as material with a compressive strength exceeding 1 MPa, consistent with the definition of the New Zealand Geomechanics Society (1988). In addition, to accommodate Australian requirements for a proposed joint Australia/New Zealand Standard for earthquake actions, rock sites were subdivided into Strong Rock Sites (Class A) and Rock Sites (Class B), with Class A sites having an unconfined compressive strength greater than 50 MPa. These two classes of sites have been retained in the new standard NZS1170.5, but for New Zealand are associated with the same spectra. The combined Strong Rock and Rock classes are referred to as Class A/B in this paper. Different attenuation expressions investigated for Strong Rock sites are not sufficiently well-constrained for publication. They are not discussed in this paper.

TABLE 3: NEW ZEALAND SITE CLASS DEFINITIONS

(now adopted in NZS1170.5:2004)

Class	Definition
Class A – Strong Rock	Strong to extremely-strong rock with: (a) unconfined compressive strength greater than 50 MPa, and (b) an average shear-wave velocity over the top 30 m greater than 1500 m/s, and (c) not underlain by materials having a compressive strength less than 18 MPa or a shear wave velocity less than 600 m/s .
Class B – Rock	Rock with: (a) a compressive strength between 1 and 50 MPa, and (b) an average shear-wave velocity over the top 30 m greater than 360 m/s, and (c) not underlain by materials having a compressive strength less than 0.8 MPa or a shear wave velocity less than 300 m/s. A surface layer of no more than 3 m depth of highly-weathered or completely-weathered rock or soil (a material with a compressive strength less than 1 MPa) may be present
Class C – Shallow Soil Sites	Sites that: (a) are not class A , class B or class E sites, and (b) have low amplitude natural period less than or equal to 0.6 s, or (c) have depths of soil not exceeding those listed in Table 4
Class D – Deep or Soft Soil Sites	Sites that: (a) are not class A , class B or class E sites, and (b) have a low-amplitude natural period greater than 0.6 s, or (c) have depths of soils exceeding those listed in Table 4, or (d) are underlain by less than 10 m of soils with an undrained shear-strength less than 12.5 kPa or soils with SPT N-values less than 6.
Class E – Very Soft Soil Sites	Sites with: (a) more than 10 m of very soft soils with undrained shear-strength less than 12.5 kPa, (b) more than 10 m of soils with SPT N values less than 6 (c) more than 10 m depth of soils with shear wave velocities of 150 m/s or less, or (d) more than 10 m combined depth of soils with properties as described in (a), (b) and (c) above.

TABLE 4: MAXIMUM DEPTH LIMITS FOR SITE SUBSOIL CLASS C

Soil type and description		Maximum depth of soil (m)
Cohesive soil	**Representative undrained shear strengths (kPa)**	
Very soft	< 12.5	0
Soft	12.5 – 25	20
Firm	25 – 50	25
Stiff	50 – 100	40
Very stiff or hard	100 – 200	60
Cohesionless soil	**Representative SPT N values**	
Very loose	< 6	0
Loose dry	6 – 10	40
Medium dense	10 – 30	45
Dense	30 – 50	55
Very dense	> 50	60
Gravels	> 30	100

The category *aL* sites were combined with the category (b) sites to form Class C, Shallow Soil Sites. Separation of the *aL* sites from rock sites and their combination with intermediate soil sites was justified by statistical studies of their residuals at an early stage of the study, and is also consistent with the classification used in the pga study of Zhao *et al.* (1997). It was found that when category *aL* sites were considered as a class on their own, their site class factors with respect to rock were non-zero for all periods, but usually not significantly different from those for category (b). The improvement in the measure-of-fit was not sufficient to justify a separate *aL* class with an extra site class term for each period. The fits were better with category *aL* sites combined with category (b) sites than with rock sites. The exact soil thickness for the transition to the *aL* category is not well constrained, in that there are few records from sites with soil thicknesses between 3 and 10 m. The important point is that the bulk of NZS4203:1992 category (a) sites with soil over rock (up to 20 m or 25 m fits category (a) for various soil types according to the description of the site class in NZS4203:1992) behave more like intermediate soil sites than like rock sites in terms of recorded earthquake motions.

Category (c) of NZS4203:1992 carried over directly into Class D, Deep or Soft Soil Sites, apart from excluding sites with at least 10 m of soil with estimated shear-wave velocities of less than 150 m/s. These sites fall into the new Class E, Very Soft Soil Sites.

Classes C and D were combined into a single "soil" class for the Zhao *et al.* pga study, but the differences in linear site-effect terms used early in the response spectrum study were found to be statistically significant at the one standard error level for all but one period (0.5s), and at the two standard error level for long periods of 1s and greater. At short periods, the site-effect term was greater for the Shallow Soil class, with a cross-over occurring between 0.5s and 0.75s, with the Deep or Soft Soil class giving stronger spectra in the long-period range. As well as the differences in the site-effect terms being statistically significant at individual periods, the

cross-over in the site-effect factors as a function of period reflects different spectral shapes for the two classes.

The New Zealand site classifications are based on site periods, generally taken as four times the estimated shear-wave travel time from rock to the surface, although generally the estimates are based on site descriptions rather than measured velocities. This approach takes account of both the type and depth of soil at a site. It differs from recent U.S. code practice of using the average shear-wave velocity to 30 m depth (V_{30}), irrespective of the depth to rock, commonly referred to as the NEHRP site classes (BSSC, 1994 and subsequent editions). The main difference occurs for deep stiff soil sites, which would be assigned to a classification associated with spectra rich in long-period content in the New Zealand classification, but to a class characterised by short-period spectra in the V_{30} approach. The classification used in this study also separates weak rock sites from shallow stiff soil sites, different from the current New Zealand Standard NZS4203:1992 and U.S. codes. Some U.S.researchers (e.g. Rodríguez-Marek *et al.*, 1999, 2000, 2001) have suggested similar modifications to the U.S. code classifications to address both these situations, based on data from the Loma Prieta and Northridge earthquakes.

The New Zealand classifications are also different from those used in the Abrahamson & Silva (1997) and Youngs *et al.* (1997) models that were the starting points for developing the New Zealand response spectrum models for crustal and subduction zone earthquakes. Abrahamson & Silva combined rock sites and sites with shallow soil up to 20 m thick in their "rock" class, which is thus intermediate between the New Zealand classes A/B and C. Their "soil" class consists of deep soil greater than 20 m thick, similar to New Zealand class D but including some class C sites as well. The Youngs *et al.* rock class is similar to New Zealand Class A/B, but their soil class is for soil greater than 20 m thickness, as in Abrahamson & Silva, with shallow stiff soil not covered by their two classes. As in the current study, records from soft soil, defined as having shear wave velocities less than 150 m/s, were excluded from the analysis.

Although there can be considerable debate about the appropriate approach to site classification, the model developed in this study has the advantage that there is a direct correspondence between the site classification scheme used and that of the proposed loadings standard, which incorporates the modifications to the NZS4203 site classes described above. To date, few U.S. attenuation relations use site classifications consistent with those used in their loadings codes, with the notable exception of the series of models summarised by Boore, Joyner & Fumal (1997). Those models use the NEHRP site classes.

The distribution of data for the four site classes by magnitude and distance is shown in Figure 5, with separate plots for crustal and subduction zone earthquakes. Open symbols are records for which only peak ground accelerations rather than spectra were used, with those at distances less than 10 km for crustal earthquakes representing the supplementary overseas pga data. There is a lack of subduction zone data at distances less than 30 km.

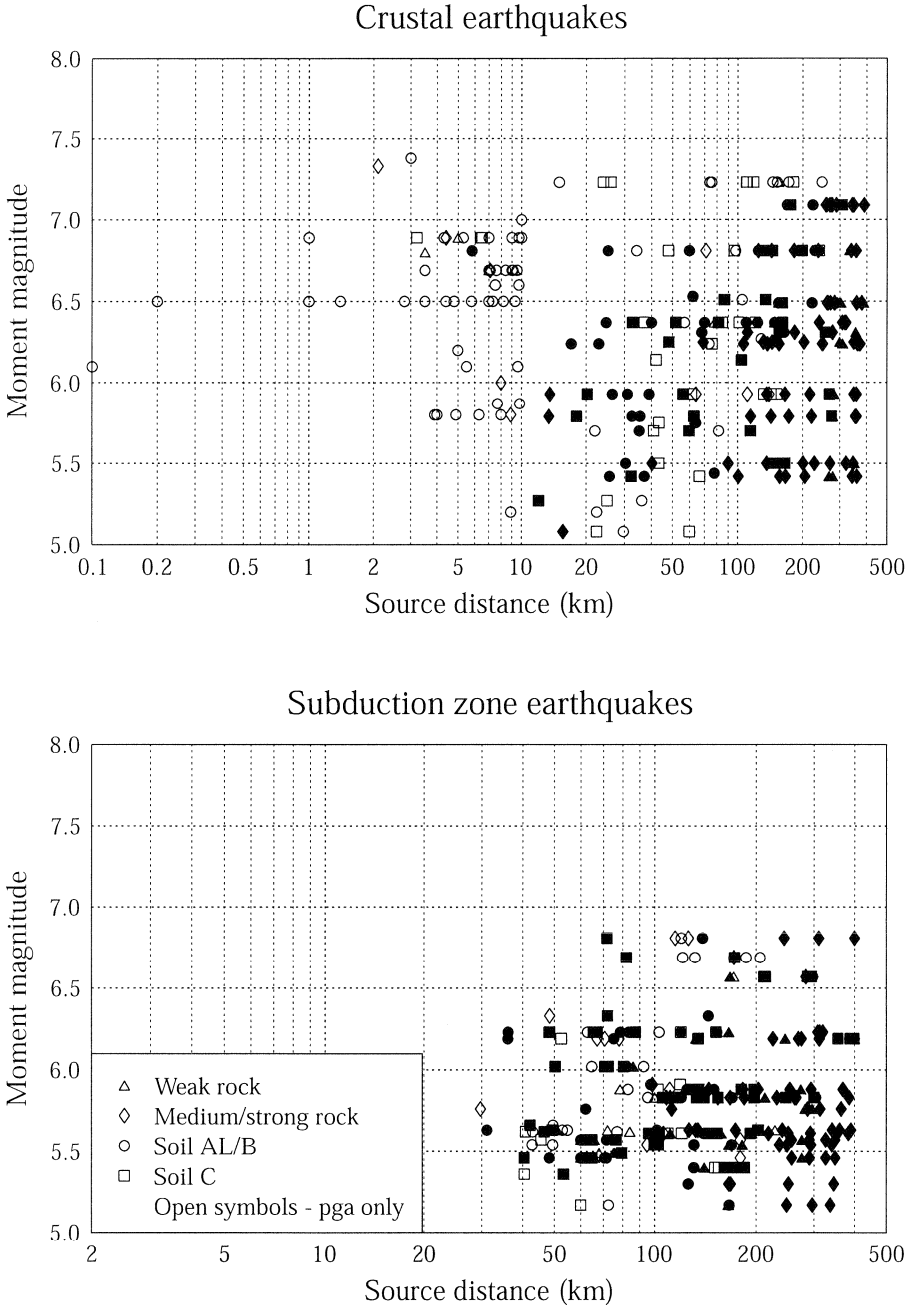

Figure 5: Distribution of data for the four site classes by magnitude and distance for (a) crustal earthquakes and (b) subduction zone earthquakes. Open symbols are records for which only peak ground accelerations were used, while solid symbols represent response spectrum data.

5. DEVELOPMENT OF THE RESPONSE SPECTRUM ATTENUATION MODEL

5.1 General Approach

A key feature of the approach in this study was to develop separate relationships for crustal, subduction interface and subduction slab earthquakes, as relationships from other parts of the world suggest that the spectra from these types of earthquake are different (Abrahamson & Shedlock, 1997; Youngs *et al.*, 1997; Atkinson & Boore, 2003). Limited

ranges of magnitude and distance and insufficient records in the SA dataset prevented the development of robust crustal and subduction zone models purely from the data. Instead, we selected as "base models" overseas attenuation models that provided reasonable matches to the New Zealand data, one for crustal earthquakes and another for subduction-zone earthquakes. The overseas base models provided the functional forms of the models, but they were modified to improve the matches to the New Zealand data

Selection of the base models was based on analyses of the residuals (i.e. the data values minus the modelled values) of the New Zealand data for various models. The models considered in the residual analyses were Abrahamson & Silva (1997), Idriss (1991), Boore *et al.* (1997) and Sadigh *et al.* (1997) for crustal earthquakes, and Youngs *et al.* (1997) and Crouse (1991) for subduction earthquakes. Some other well-known models were eliminated because they developed a single model for both crustal and subduction zone earthquakes (e.g. the Japanese models of Fukushima & Tanaka, 1990; and Molas & Yamazaki, 1995). The crustal earthquake models of Campbell (1997) and Boore *et al.* (1997) failed to satisfy a criterion that they cover distances to at least 150 km from the source, imposed to provide sufficient New Zealand data for the analyses

Figures 6a and 6b show residuals of ln(SA) for soil sites for the Abrahamson and Silva (1997) crustal-earthquake model, and for rock and soil sites for the Youngs *et al.* (1997) subduction-zone model. All four crustal models gave adequate fits to the New Zealand data, as shown in Figure 6a for deep soil sites for the Abrahamson & Silva model. Both subduction zone models matched the deep-slab data well, but were poor for the New Zealand interface and shallow-slab data, over-predicting at short periods, and under-predicting at long periods, as shown for the Youngs *et al.* model in Figure 6b.

The Abrahamson and Silva (1997) (A&S) model was selected as the base model for crustal earthquakes, and the Youngs *et al.* (1997) model as the base model for subduction zone earthquakes. The crustal and subduction zone expressions that have been developed from these base models are linked through common site response terms and standard deviations. This link has been used to provide a more robust definition of these terms.

Constraints were imposed so that the base models provided the values of model coefficients that are reliant for their reliable estimation on data from ranges of magnitude, distance, or other model parameters that are sparsely represented in the New Zealand data. In the final models, the overseas models were used to provide constraints on coefficients that affect the estimates for the near-source region, to determine the coefficients of the source-mechanism terms for crustal earthquakes, and to specify the hanging-wall term for crustal earthquakes. Some terms in the base models were eliminated, because statistical testing showed that they had little effect on the measures of fit. The coefficients of other terms were determined in regression analyses to provide maximum likelihood matches to the New Zealand data.

(a) Abrahamson & Silva (1997) relationship for crustal earthquakes

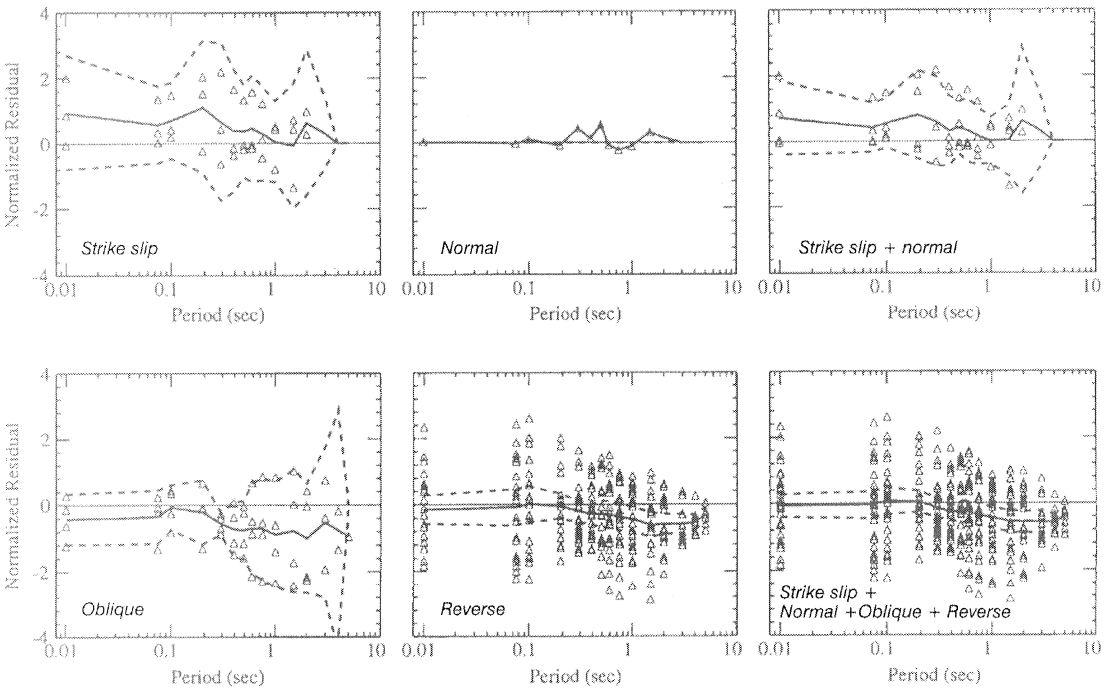

(b) Youngs et al. (1997) relationship for intraslab and interface earthquakes

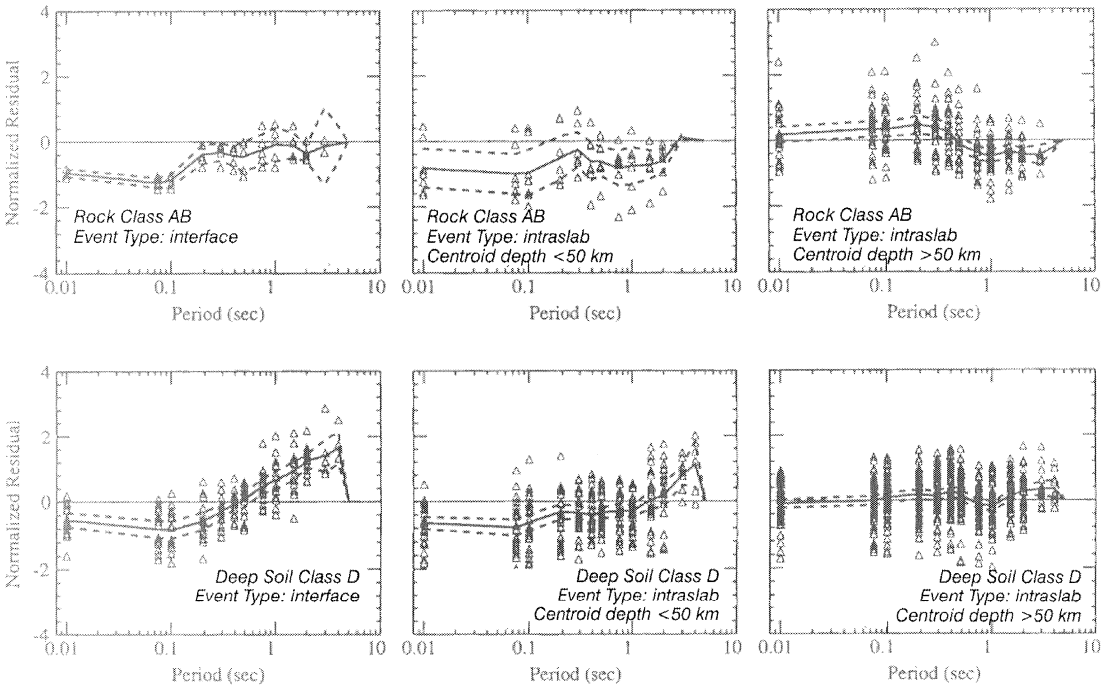

Figure 6: Residuals between (a) the Abrahamson & Silva model and New Zealand crustal data for deep soil sites and (b) the Youngs et al. model and New Zealand subduction zone data for rock and deep soil sites.

5.2 Regression Methodology

The regression analysis was performed using software provided by Abrahamson that implements the Abrahamson & Youngs (1992) random-effects algorithm, a maximum likelihood method that accounts for correlations in the data recorded from a single earthquake. It overcomes some of the difficulties of estimating coefficient values for strongly-correlated terms. Others (e.g. Joyner & Boore (1981), Boore *et al.* (1997), Fukushima & Tanaka, 1990; Molas & Yamazaki, 1995) have tackled these difficulties through two-step regressions, in one step determining the attenuation with distance within earthquakes and in the other considering the dependence on magnitude.

Since the random-effects model considers the correlation of data within an event, it has two error terms: an intra-event (within-earthquake) residual and an inter-event (between-earthquake) residual. The inter-event residual is the event term which represents the common residual (i.e. error) for all records from the same earthquake. The intra-event residuals show the variability in the ground motion from the predicted values after the event term has been removed.

5.3 Statistical criteria for eliminating or constraining parameters

In modifying existing models to obtain "better" fits to New Zealand data, it is necessary to have clearly defined criteria to determine what is regarded as an improved model. The measures-of-fit of the modelled response spectrum accelerations to the data were expressed primarily in terms of their log-likelihoods, LL, defined for the random-effects model in the Appendix.

It became apparent that quite substantial changes in the values of many coefficients of the model could be offset by changes in the values of other coefficients so that there was little overall change in the measure-of-fit, LL, to the data. This behaviour is symptomatic of models containing more terms than can be adequately constrained by the data. Consequently, a systematic attempt was made to reduce the number of terms in the model to obtain a more robust fit to the data, using other statistical criteria (see Appendix). In particular, minimization of the value of the Akaike Information Criterion (AIC) (Akaike, 1974) was found to be useful in determining a "parsimonious" set of parameters to be included in the models. The AIC adds a penalty term to the LL based on the number of fitted coefficients, such that a reduction in the number of parameters by one constitutes a better model if the corresponding reduction in the LL value is less than 1.0.

All terms constrained or deleted from the preliminary model have been justified on a statistical basis, but in some cases terms have been retained because of other considerations despite the tests indicating that their inclusion was not statistically significant.

6. FINAL MODELS

The attenuation models developed in this study were based on the Abrahamson & Silva (1997) model for crustal earthquakes and the Youngs *et al.* (1997) model for subduction zone earthquakes. As a result, the forms of the crustal earthquake and subduction zone earthquake expressions are similar to those models.

The model development was performed for the larger horizontal component. Results are also given for the geometric mean of the horizontal components, for which it was assumed that the same model form is appropriate.

First, expressions giving intermediate values $SA'_{A/B,C,D}(T)$ of the response spectrum accelerations and $PGA'_{A/B,C,D}$ of the peak ground accelerations for each of the site classes *A/B*, *C* and *D* were developed from the dataset *QKE9_ALL.TXT* that includes only those records for which response spectra are available. Then peak ground accelerations $PGA_{A/B,C,D}$ were obtained by regression from the complete pga data set *PGA6F5AC.TXT*, including those records for which response spectra were not available. Finally, the intermediate values $SA'_{A/B,C,D}(T)$ of the response spectrum accelerations were multiplied by the ratio $PGA_{A/B,C,D} / PGA'_{A/B,C,D}$ of the peak

ground accelerations for the two models obtained from the two datasets to obtain the values $SA_{A/B,C,D}(T)$ which together with the pga model $PGA_{A/B,C,D}$ from the larger dataset provide the recommended model from this study. The reason for the multiplication by the pga ratio is that for some subsets of earthquake motions, notably on rock or deep soil sites for crustal earthquakes, the pga estimates $PGA'_{A/B,C,D}$ from the response spectrum dataset were considerably smaller than the estimates $PGA_{A/B,C,D}$ derived from the complete pga dataset, particularly near-source. As the $PGA_{A/B,C,D}$ values were more in line with those from models from western US data, it was decided to scale the $SA'(T)$ values by the ratio of the pgas from the two models to obtain the final values of $SA(T)$, even though this introduces a bias to the final model with respect to the New Zealand data. Note that this scaling applies for the particular set of independent parameters (magnitude, distance, mechanism, tectonic class, site class) that applies in a particular case, so varies continuously as a function of these parameters. For parameter combinations where the models are well constrained by the data so that the pga estimates are similar for the two models, the scaling by the pga ratio has little effect. For parameter values, such as at short distances, where the $PGA'_{A/B,C,D}$ values are poorly constrained, the scaling may be more substantial. The standard deviations are taken as those with from the regression analyses, with no modification to account for any bias introduced by the pga scaling procedure.

The crustal model takes the form:

$$\begin{aligned}\ln SA'_{A/B}(T) = {} & \mathbf{C_1'(T)} + C_{4AS}(M-6) \\ & + C_{3AS}(T)\,(8.5-M)^2 \\ & + \mathbf{C_5'(T)}\, r + (\mathbf{C_8'(T)} \\ & + C_{6AS}(M-6))\,\ln(r^2 + C_{10AS}^2(T))^{1/2} \\ & + \mathbf{C_{46}'(T)}\, r_{VOL} \\ & + C_{32}\, CN + C_{33AS}(T)\, CR + F_{HW}(M,r)\end{aligned} \qquad (1)$$

The subduction zone model takes the form:

$$\begin{aligned}\ln SA'_{A/B}(T) = {} & \mathbf{C_{11}'(T)} + (C_{12Y} + (C_{15}'(T) \\ & - \mathbf{C_{17}'(T)})\, C_{19Y}\,)\,(M-6) \\ & + C_{13Y}(T)(10-M)^3 \\ & + \mathbf{C_{17}'(T)}\,\ln(r + C_{18Y}\exp(C_{19Y}\,M)) \\ & + \mathbf{C_{20}'(T)}\, H_C + \mathbf{C_{24}'(T)}\, SI \\ & + \mathbf{C_{46}'(T)}\, r_{VOL}\,(1-DS)\end{aligned} \qquad (2)$$

where

$$C_{15}'(T) = C_{17Y}(T) \qquad (3)$$

In both the crustal and subduction zone models

$$\begin{aligned}\ln SA'_{C,D}(T) = {} & \ln SA'_{A/B}(T) + \mathbf{C_{29}'(T)}\,\delta_C \\ & + (C_{30AS}(T)\,\ln(PGA'_{A/B}+0.03) \\ & + \mathbf{C_{43}'(T)})\,\delta_D\end{aligned} \qquad (4)$$

where

$$PGA'_{A/B} = SA'_{A/B}(T=0) \qquad (5)$$

The expressions for $PGA_{A/B,C,D}$ take the same form as those for $PGA'_{A/B,C,D}$, but are differentiated by using unprimed versions of the coefficients. Finally,

$$\begin{aligned}SA_{A/B,C,D}(T) = {} & SA'_{A/B,C,D}(T) \\ & * (\,PGA_{A/B,C,D} / PGA'_{A/B,C,D}\,)\end{aligned} \qquad (6)$$

The complicated form of the coefficient of the magnitude term for subduction-zone earthquakes results from applying a near-source constraint at distance $r=0$. The magnitude-dependence of the model is constrained to be the same as that of the Youngs *et al.* model at zero distance, to retain the same degree of magnitude saturation at zero distance. This constraint is discussed further in Section 6.3. Note that although the coefficients $C_{15}'(T)$ are the same as $C_{17Y}(T)$, and the subduction zone expression is perhaps easier to understand with this substitution made, this notation is used so as to identify where the values are listed in Tables 5 and 6. The notation C_{12Y} and $C_{17Y}(T)$ is used to indicate the coefficients of the $(M-6)$ and $ln(distance)$ terms respectively in the Youngs *et al.* expression.

The parameters of these models are:

M = moment magnitude

r = shortest distance in km from the site to source

r_{VOL} = length in km of the part of the source-to-site path in

the volcanic zone (see Section 9.1)

H_C = centroid depth in km

CN = -1 for normal mechanism crustal earthquakes, 0 otherwise

CR = 0.5 for reverse/oblique mechanism crustal earthquakes, 1.0 for reverse mechanism crustal earthquakes, 0 otherwise

The source mechanisms are defined in terms of rake angle at the end of Section 2.2.

$F_{HW}(M,r)$ = hanging wall factor of the Abrahamson & Silva model (see Section 6.1).

SI = 1 for subduction interface earthquakes, 0 otherwise

DS = 1 for deep slab earthquakes, 0 otherwise

Interface and subduction slab earthquakes are defined in Section 2.1

δ_C = 1 for site class C, 0 otherwise

δ_D = 1 for site class D, 0 otherwise

$C_i(0)$ and $C'_i(T)$ = coefficients of the attenuation model, listed in Tables 5 & 6.

TABLE 5: COEFFICIENTS OF THE ATTENUATION MODEL P2MRF5AC FOR THE STRONGER HORIZONTAL COMPONENT

period	0.000	0.000	0.075	0.10	0.20	0.30	0.40	0.50	0.75	1.00	1.50	2.00	3.00	
1	0.28815	0.18130	1.36561	1.77717	1.39535	0.44591	0.01645	0.14826	-0.21246	-0.10451	-0.48665	-0.77433	-1.30916	free
3	0.00000	0.00000	0.03000	0.02800	-0.01380	-0.03600	-0.05180	-0.06350	-0.08620	-0.10200	-0.12000	-0.12000	-0.17260	fixed
4	-0.14400	-0.14400	-0.14400	-0.14400	-0.14400	-0.14400	-0.14400	-0.14400	-0.14400	-0.14400	-0.14400	-0.14400	-0.14400	fixed
5	-0.00967	-0.00846	-0.00889	-0.00837	-0.00940	-0.00987	-0.00923	-0.00823	-0.00738	-0.00588	-0.00630	-0.00630	-0.00553	free
6	0.17000	0.17000	0.17000	0.17000	0.17000	0.17000	0.17000	0.17000	0.17000	0.17000	0.17000	0.17000	0.17000	fixed
8	-0.70494	-0.75519	-0.94568	-1.01852	-0.78199	-0.56098	-0.51281	-0.56716	-0.55384	-0.65892	-0.58222	-0.58222	-0.57009	free
10	5.60000	5.60000	5.58000	5.50000	5.10000	4.80000	4.52000	4.30000	3.90000	3.70000	3.55000	3.55000	3.50000	fixed
11	8.68354	8.10697	8.68782	9.37929	10.61479	9.40776	8.50343	8.46463	7.30176	7.08727	6.93264	6.64496	5.05488	free
12	1.41400	1.41400	1.41400	1.41400	1.41400	1.41400	1.41400	1.41400	1.41400	1.41400	1.41400	1.41400	1.41400	fixed
13	0.00000	0.00000	0.00000	-0.00110	-0.00270	-0.00360	-0.00430	-0.00480	-0.00570	-0.00640	-0.00730	-0.00730	-0.00890	fixed
15	-2.55200	-2.55200	-2.70700	-2.65500	-2.52800	-2.45400	-2.40100	-2.36000	-2.28600	-2.23400	-2.16000	-2.16000	-2.03300	fixed
17	-2.56727	-2.48795	-2.54215	-2.60945	-2.70851	-2.47668	-2.36895	-2.40630	-2.26512	-2.27668	-2.28347	-2.28347	-2.03050	free
18	1.78180	1.78180	1.78180	1.78180	1.78180	1.78180	1.78180	1.78180	1.78180	1.78180	1.78180	1.78180	1.78180	fixed
19	0.55400	0.55400	0.55400	0.55400	0.55400	0.55400	0.55400	0.55400	0.55400	0.55400	0.55400	0.55400	0.55400	fixed
20	0.01550	0.01622	0.01850	0.01740	0.01542	0.01278	0.01426	0.01287	0.01080	0.00946	0.00788	0.00788	-0.00265	free
24	-0.50962	-0.41369	-0.48652	-0.61973	-0.67672	-0.59339	-0.30579	-0.24839	-0.01298	0.06672	-0.02289	-0.02289	-0.20537	free
29	0.30206	0.44307	0.31139	0.34059	0.37235	0.56648	0.69911	0.63188	0.51577	0.34048	0.12468	0.12468	0.14593	free
30	-0.23000	-0.23000	-0.28000	-0.28000	-0.24500	-0.19500	-0.16000	-0.12100	-0.05000	0.00000	0.04000	0.04000	0.04000	fixed
32	0.20000	0.20000	0.20000	0.20000	0.20000	0.20000	0.20000	0.20000	0.20000	0.20000	0.20000	0.20000	0.20000	fixed
33	0.26000	0.26000	0.26000	0.26000	0.26000	0.19800	0.15400	0.11900	0.05700	0.01300	-0.04900	-0.04900	-0.15600	fixed
43	-0.31769	-0.29648	-0.48366	-0.43854	-0.29906	-0.05184	0.20301	0.37026	0.73517	0.87764	0.75438	0.75438	0.61545	free
46	-0.03279	-0.03301	-0.03452	-0.03595	-0.03853	-0.03604	-0.03364	-0.03260	-0.02877	-0.02561	-0.02034	-0.02034	-0.01673	free
SigmaM6	0.4865	0.5035	0.5281	0.5398	0.5703	0.5505	0.5627	0.5680	0.5562	0.5629	0.5394	0.5394	0.5701	
Sigslope	-0.1261	-0.0635	-0.0970	-0.0673	-0.0243	-0.0861	-0.1405	-0.1444	-0.0932	-0.0749	-0.0056	-0.0056	0.0934	
Tau	0.2687	0.2598	0.3217	0.3088	0.2726	0.2112	0.2005	0.1476	0.1794	0.2053	0.2411	0.2411	0.2406	
SigtotM6	0.5558	0.5666	0.6184	0.6219	0.6321	0.5896	0.5973	0.5869	0.5844	0.5992	0.5909	0.5909	0.6188	

Model P2MRF5AC

TABLE 6: COEFFICIENTS FOR GEOMETRIC-MEAN OF THE 5% DAMPED ACCELERATION RESPONSE SPECTRA COMPONENTS

period	0.000	0.000	0.075	0.10	0.20	0.30	0.40	0.50	0.75	1.00	1.50	2.00	3.00	
1	0.14274	0.07713	1.22050	1.53365	1.22565	0.21124	-0.10541	-0.14260	-0.65968	-0.51404	-0.95399	-1.24167	-1.56570	free
3	0.00000	0.00000	0.03000	0.02800	-0.01380	-0.03600	-0.05180	-0.06350	-0.08620	-0.10200	-0.12000	-0.12000	-0.17260	fixed
4	-0.14400	-0.14400	-0.14400	-0.14400	-0.14400	-0.14400	-0.14400	-0.14400	-0.14400	-0.14400	-0.14400	-0.14400	-0.14400	fixed
5	-0.00989	-0.00898	-0.00914	-0.00903	-0.00975	-0.01032	-0.00941	-0.00878	-0.00802	-0.00647	-0.00713	-0.00713	-0.00623	free
6	0.17000	0.17000	0.17000	0.17000	0.17000	0.17000	0.17000	0.17000	0.17000	0.17000	0.17000	0.17000	0.17000	fixed
8	-0.68744	-0.73728	-0.93059	-0.96506	-0.75855	-0.52400	-0.50802	-0.52214	-0.47264	-0.58672	-0.49268	-0.49268	-0.52257	free
10	5.60000	5.60000	5.58000	5.50000	5.10000	4.80000	4.52000	4.30000	3.90000	3.70000	3.55000	3.55000	3.50000	fixed
11	8.57343	8.08611	8.69303	9.30400	10.41628	9.21783	8.01150	7.87495	7.26785	6.98741	6.77543	6.48775	5.05424	free
12	1.41400	1.41400	1.41400	1.41400	1.41400	1.41400	1.41400	1.41400	1.41400	1.41400	1.41400	1.41400	1.41400	fixed
13	0.00000	0.00000	0.00000	-0.00110	-0.00270	-0.00360	-0.00430	-0.00480	-0.00570	-0.00640	-0.00730	-0.00730	-0.00890	fixed
15	-2.55200	-2.55200	-2.70700	-2.65500	-2.52800	-2.45400	-2.40100	-2.36000	-2.28600	-2.23400	-2.16000	-2.16000	-2.03300	fixed
17	-2.56592	-2.49894	-2.55903	-2.61372	-2.70038	-2.47356	-2.30457	-2.31991	-2.28460	-2.28256	-2.27895	-2.27895	-2.05560	free
18	1.78180	1.78180	1.78180	1.78180	1.78180	1.78180	1.78180	1.78180	1.78180	1.78180	1.78180	1.78180	1.78180	fixed
19	0.55400	0.55400	0.55400	0.55400	0.55400	0.55400	0.55400	0.55400	0.55400	0.55400	0.55400	0.55400	0.55400	fixed
20	0.01545	0.01590	0.01821	0.01737	0.01531	0.01304	0.01426	0.01277	0.01055	0.00927	0.00748	0.00748	-0.00273	free
24	-0.49963	-0.43223	-0.52504	-0.61452	-0.65966	-0.56604	-0.33169	-0.24374	-0.01583	0.02009	-0.07051	-0.07051	-0.23967	free
29	0.27315	0.38730	0.27879	0.28619	0.34064	0.53213	0.63272	0.58809	0.50708	0.33002	0.07445	0.07445	0.09869	free
30	-0.23000	-0.23000	-0.28000	-0.28000	-0.24500	-0.19500	-0.16000	-0.12100	-0.05000	0.00000	0.04000	0.04000	0.04000	fixed
32	0.20000	0.20000	0.20000	0.20000	0.20000	0.20000	0.20000	0.20000	0.20000	0.20000	0.20000	0.20000	0.20000	fixed
33	0.26000	0.26000	0.26000	0.26000	0.26000	0.19800	0.15400	0.11900	0.05700	0.01300	-0.04900	-0.04900	-0.15600	fixed
43	-0.33716	-0.31036	-0.49068	-0.46604	-0.31282	-0.07565	0.17615	0.34775	0.72380	0.89239	0.77743	0.77743	0.60938	free
46	-0.03255	-0.03250	-0.03441	-0.03594	-0.03823	-0.03535	-0.03354	-0.03211	-0.02857	-0.02500	-0.02008	-0.02008	-0.01587	free
SigmaM6	0.4871	0.5099	0.5297	0.5401	0.5599	0.5456	0.5556	0.5658	0.5611	0.5573	0.5419	0.5419	0.5809	
Sigslope	-0.1011	-0.0259	-0.0703	-0.0292	0.0172	-0.0566	-0.1064	-0.1123	-0.0836	-0.0620	0.0385	0.0385	0.1403	
Tau	0.2677	0.2469	0.3139	0.3017	0.2583	0.1967	0.1802	0.1440	0.1871	0.2073	0.2405	0.2405	0.2053	
SigtotM6	0.5558	0.5666	0.6157	0.6187	0.6166	0.5800	0.5840	0.5839	0.5915	0.5946	0.5929	0.5929	0.6161	

Model GMMRFTMP

The coefficients in Table 5 give $PGA_{A/B,C,D}$, $PGA'_{A/B,C,D}$ and $SA'_{A/B,C,D}(T)$ values that are the 50-percentile (i.e. median) values of the larger of two randomly-oriented but orthogonal horizontal components of the 5% damped response spectral acceleration in g at period T for site class *A/B*, *C* or *D*. The coefficients in Table 6 lead to the 50-percentile values of the geometric mean of the two components. The first column for $T=0s$ gives the coefficients for $PGA_{A/B,C,D}$ from the larger dataset including all pga records. The second column for $T=0s$ gives the coefficients for $PGA'_{A/B,C,D}$ from the smaller dataset for which there are response spectra. The subsequent columns for $T=0.075s$ to $T=3s$ list the coefficients for $SA'_{A/B,C,D}(T)$. The final values $SA_{A/B,C,D}(T)$ are obtained by multiplying $SA'_{A/B,C,D}(T)$ by the pga ratio $PGA_{A/B,C,D}$ / $PGA'_{A/B,C,D}$, as indicated in equation (6).

The three rows in Tables 5 and 6 following the $C_{46}'(T)$ coefficients list the parameters σ_{M6} (*SigmaM6*), *Sigslope* and τ (*Tau*) associated with the standard deviations $\sigma_{total}(M_w, T)$ of the logarithm of the response spectrum acceleration, *lnSA(T)*, as presented in Section 6.6. The final row *SigtotM6* serves as a check of the correct implementation of the standard deviation expressions, giving the value of $\sigma_{total}(M_w=6, T)$ (see equation 9 in Section 6.6).

The distance r is intended to represent the shortest distance to the source. For those ten New Zealand events where a model of the rupture surface was available, the slant distance from the recording site to the closest point on the rupture surface was taken. For remaining events, r was taken as the slant distance from the site to the centroid of the rupture surface. Most of this second type of distance data is unlikely to be sensitive to the use of the centroid rather than the (unknown) closest point on the rupture surface, as the dimensions of most of the rupture surfaces would have been relatively small compared to the slant distances. In only five instances was this discrepancy likely to have been more than 10 percent (Zhao *et al.*, 1997). The depth used here is the "centroid depth" (H_C). The "centroid depth" is the standard depth determined in focal mechanism and moment determinations (e.g. Dziewonski *et al.*, 1983; Webb & Anderson, 1998; Dowrick & Rhoades, 1998).

Free coefficients in the regressions are shown in bold in the expressions above, and comprise only a small proportion of the coefficients in the models. The free coefficients consist of the "constant" terms for both the crustal and subduction zone models ($C_1(T)$ and $C_{11}(T)$), the ln(distance term) coefficients ($C_8(T)$ and $C_{17}(T)$), the anelastic attenuation coefficients ($C_5(T)$ and $C_{46}(T)$), the depth and interface coefficients for the subduction zone ($C_{20}(T)$ and $C_{24}(T)$), and the linear site terms, $C_{29}(T)$ and $C_{43}(T)$.

Coefficients subscripted $_{AS}$ take the same values as the equivalent coefficients in the Abrahamson & Silva model, while those subscripted $_Y$ take values of the Youngs *et al.* rock model. Some of these coefficients were allowed to vary from the Abrahamson & Silva or Youngs *et al.* values during development of the model, but the resulting changes were demonstrated to be statistically insignificant by various of the tests discussed in the Appendix. Although the possibility of varying nonlinearly occurring coefficients such as $C_{10}(T)$ from their Abrahamson & Silva values was investigated to a limited extent, this could be implemented only by time-consuming and tedious trial-and-error iteration. Modified values of these coefficients appeared to make little difference to the measure-of-fit. Accordingly, nonlinearly occurring parameters were constrained to their values in the pre-existing models.

The equations apply for moment magnitudes of about 5.25 to 7.5, and distances up to 400 km, corresponding approximately to the magnitude and distance ranges of the data used in the regressions. Care should be taken also in applying the equations for earthquakes of depth greater than 150 km, with some restrictions recommended for such earthquakes (see Section 11.2). There are also problems with the model for magnitudes less than 5.25, as explained in Section 11.1. The model was fitted for 12 periods, ranging from 0s (corresponding to pga) to 3s. The 12 periods are those for which the Youngs *et al.* model is defined, namely 0s, 0.075s, 0.1s, 0.2s, 0.3s, 0.4s, 0.5s, 0.75s, 1.0s, 1.5s, 2.0s and 3.0s. The Abrahamson & Silva model is defined for a more closely spaced set of periods which in addition extends to 5s. The magnitude and distance range are more limited

than those of the Youngs et al model, which includes data from earthquakes up to magnitude 8 and applies for distances up to 500 km. The Abrahamson & Silva model is based on data from earthquakes between magnitudes 4.4 and 7.4, for distances ranging from 0.1 km to about 250 km.

6.1 Hanging Wall Factor

There is a systematic increase in the motions on the hanging wall compared to those on the foot wall of dipping faults at the same distance from the rupture plane. To consider this effect, the Abrahamson & Silva (1997) hanging wall term is appropriate to use in conjunction with the present model, as indicated by the $F_{HW}(M,R)$ term in equation (1). This term has full effect for distances between 4 km and 18 km from the rupture, with some effect for distances from 0 km to 25 km from the rupture for sites on the hanging wall of a fault. There are few response spectrum data from crustal reverse-mechanism earthquakes within this distance range in the current study. Accordingly, this effect has not been modelled in the regression analysis.

6.2 Magnitude saturation

Both the crustal and subduction earthquake attenuation expressions exhibit "magnitude saturation" at short distances i.e. they have less dependence on magnitude at short distances than they do at large distances, especially for motions of short spectral periods. This behaviour is carried through from the Abrahamson & Silva and Youngs *et al.* models. It is a feature of many modern attenuation models, and requires the shapes of the attenuation curves to be dependent on magnitude.

The basis of the argument for near-source magnitude-saturation is summarised by Bolt and Abrahamson (1982):

"..high-frequency (>8 Hz) spikes of acceleration near to the source are predominantly generated by local dislocation or rapid slip on fault surfaces and not remote dislocation along the rupturing fault. The amplitudes of peak accelerations with high frequencies are governed by these local stress drops and rock properties rather than by the average dynamical fault properties that depend upon overall rupture dimensions. This physical model of wave generation discounts the influence of magnitude (or seismic moment) on the supremum acceleration at a particular site..."

The Abrahamson & Silva and Youngs *et al.* models use different functional forms to obtain magnitude-saturation. Youngs *et al.* use a common form of model, with a magnitude-increasing term added to the distance in the ln distance term (e.g. Youngs *et al.*, 1988; Crouse, 1991; Sadigh *et al.*, 1997). The Abrahamson & Silva model instead uses a magnitude-dependent slope of the ln(distance) term. These different forms of model produce different transitions between the attenuation curves at short and long distances. In the form with additive magnitude-dependent distances, the attenuation curves start diverging noticeably from the zero-distance values at distances that increase with magnitude, with the slopes of the attenuation curves tending to the same value for all magnitudes at large distances. The curves for different magnitudes diverge with increasing distance at short distances, but become "parallel" at large distances. In the alternative Abrahamson & Silva form, the magnitude-dependent slopes of the ln(distance) terms cause the curves for different magnitudes to continue diverging at all distances.

The Youngs *et al.* model has total magnitude saturation (i.e. no dependence on magnitude) at zero distance. However, their data from subduction earthquakes do not include distances shorter than 8.5 km for interface earthquakes, and less than about 50 km for intraslab earthquakes. For crustal earthquakes, magnitude saturation is physically significant, as source-to-site distances can be very short for surface-rupturing faults. However, there is a lack of the same physical significance for saturation in subduction zone earthquakes, because distances approaching zero never occur. Nevertheless, Youngs *et al.* (1988) report that their subduction earthquake data exhibit a degree of saturation of near-source ground motions.

6.3 Near-source constraints

The New Zealand data are sufficient to determine the

magnitude dependence at distances beyond about 20 km to 30 km from the source, except for large magnitudes of 7.3 or greater, but are lacking in the near-source zone where magnitude-saturation has effect. The near-source magnitude-dependence was determined by imposing constraints in this study to require that the crustal and subduction zone expressions for rock sites match the magnitude-dependence of the Abrahamson & Silva and Youngs *et al.* models respectively at zero distance *(r=0)*. Also, these constraints require that the coefficients of the quadratic magnitude term for crustal earthquakes are the same as for Abrahamson & Silva, i.e. $C_3(T)=C_{3AS}(T)$, and that the cubic magnitude term are the same as in the Youngs *et al.* model for subduction earthquakes.

As a special case, setting all parameters occurring in the near-source constraint expressions to their Abrahamson & Silva or Youngs *et al.* values satisfies the constraints, and may be appropriate if either the pairs of values, $C_4(T)$ and $C_6(T)$ or $C_{12}(T)$ and $C_{17}(T)$, of the unconstrained parameters determined from the linear regression or the associated measures-of-fit of the model differ insignificantly from their default values. The equation for the crustal New Zealand model (equation 1) reflects this situation for larger magnitude earthquakes ($M > 6.4$), with C_4 and C_6 both taken as the Abrahamson & Silva values.

For the subduction zone case, the change in $C_{17}(T)$ from $C_{17Y}(T)$ was found to be significant, so the constrained variation was allowed. This led to the single value for all periods of the coefficient C_{12Y} of the linear-magnitude term being replaced by period-dependent coefficients $C_{12}^*(T)$. There were associated changes in the coefficients $C_{17}(T)$ of the *ln(distance term)*. The coefficients of these two terms are linked through the $r=0$ near-source constraint that the magnitude-dependence is the same as for the Youngs *et al.* (1997) model at $r=0$:

$$C_{12}^*(T) = C_{12Y} + (C_{17Y}(T) - C_{17}(T))\, C_{19Y} \qquad (7)$$

With this constraint, which explains the complicated form of the magnitude term in equation (2), the model retains complete saturation for pga at $r=0$, as in the Youngs *et al.* model. It also retains the period-dependent degree-of-saturation of the Youngs *et al.* model for other periods.

6.4 Near-source directivity and polarisation effects

There are systematic near-source effects that are not accounted for by most attenuation models, including those developed in this study. Directivity of the rupture propagation process causes the amplitudes of the motion to be significantly enhanced when most of the rupture propagation occurs towards the site, and to be reduced for sites away from the direction of the rupture propagation. Strong polarisation often occurs in near-source motions, irrespective of the degree of directivity, with the medium- to long-period components of motion being stronger in the direction perpendicular to the strike of the fault. These two effects can be taken into account by modifying the standard estimates using factors given by Somerville *et al.* (1997), and it is recommended that these factors should be applied when estimating spectra for individual near-fault sites. In the Somerville *et al.* model, the maximum near-fault factors increase with period from 1.0 at a period of 0.5s, although they are not significant for periods less than about 1.5s.

The Somerville *et al.* rupture-directivity factors are applicable for the New Zealand attenuation model presented here in that Somerville *et al.* state that "they may provide approximate adjustment factors for other attenuation relations that use similar definitions of parameters such as rupture distance and that have similar functional forms" to the Abrahamson and Silva (1997) attenuation model for which they were derived.

Polarisation is modelled using factors representing the ratios of the fault-normal to fault-parallel motions. These were determined directly from recorded data, and so are independent of a particular attenuation model. However, as the factors are with respect to the geometric mean values of the two horizontal components, they need to be used in conjunction with the geometric mean form of the New Zealand model, or else a further adjustment needs to be

applied to account for the ratio between the larger and geometric-mean component values.

6.5 Linking of crustal and subduction zone models

The crustal and subduction zone expressions are linked through common site effect terms (Section 8), which are a function of estimated median rock pga and spectral period. The Abrahamson & Silva model treated site effects through terms of the same form used in the current model, but with fewer site classes. Youngs *et al.* accommodated site effects through different coefficient values for rock and soil sites, subject to some zero-distance constraints. The subduction zone expressions for the current model are based on the Youngs *et al.* rock expressions, with site effects accounted for by terms of the Abrahamson & Silva type. The two sets of expressions also share common standard deviations.

6.6 Standard Deviations

The standard deviation $\sigma_{total}(M_w, T)$ of the estimate *lnSA(T)* for each period are composed of inter-event and intra-event terms, as discussed in section 5.2. They are assumed independent for different spectral periods, but are applied to the overall data for each spectral period, without separation for such parameters as site class or tectonic class of earthquake. The intra-event component $\sigma_{intraevent}(M_w,T)$ is magnitude-dependent, while theinter-event standard error $\tau(T)$ is independent of magnitude.

The partitioning of the standard deviation between the two components is a consequence of the random-effects methodology applied for regression analysis. The dependence on magnitude is a feature of several modern attenuation models (e.g. Abrahamson & Silva (1997); Youngs *et al.* (1997); Sadigh *et al.* (1997); Campbell (1997)), although some have magnitude-dependence of both components of the variance.

The $\sigma_{intraevent}(M_w,T)$ are defined in terms of their values at magnitude M_w 6, $\sigma_{M6}(T)$, and their slopes with magnitude, *Sigslope(T)*.

$$\sigma_{intraevent}(M_w,T) = \sigma_{M6}(T) + Sigslope(T) * (M_w - 6) \quad \text{for } 5 < M_w < 7 \qquad (8a)$$

$$\sigma_{intraevent}(M_w<5, T) = \sigma_{M6}(T) - Sigslope(T) \qquad (8b)$$

$$\sigma_{intraevent}(M_w>7, T) = \sigma_{M6}(T) + Sigslope(T) \qquad (8c)$$

The total standard error is the square root of the sum of the squares of the inter- and intra-event standard error, i.e. the total variance is the sum of the inter- and intra- event variances.

$$\sigma_{total}(M_w, T) = sqrt\ (\ \sigma_{intraevent}(M_w,T)^2 + \tau(T)^2\ ) \qquad (9)$$

The values of the parameters σ_{M6} (*SigmaM6)*, *Sigslope* and τ *(Tau)* are presented in the final few lines of Tables 5 and 6.The values *SigtotM6* presented in the final row of each of these Tables serves as a check of the correct implementation of the standard deviation expressions, giving the value of $\sigma_{total}(M_w=6, T)$ (see equation 9).

A pleasing result is that the standard errors are generally similar to those of the Abrahamson & Silva model and much smaller than those of the Youngs *et al.* model (e.g. Figure 7), meaning that the match of the modified models to the supplemented New Zealand dataset is generally better than achieved by the original models to the data from which they were derived.

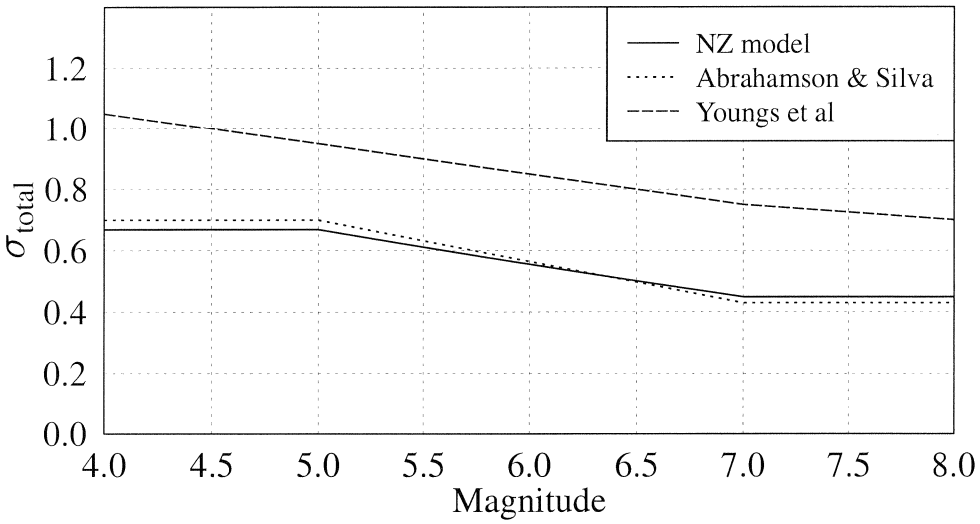

Figure 7: Total standard errors σ_{total} as a function of magnitude for New Zealand and base models for ln(pga).

7. MODIFICATIONS OF THE BASE MODELS

The Abrahamson & Silva and Youngs *et al.* models have been modified to obtain improved matches to the New Zealand data. Some changes involved obtaining different coefficient values from the regression analyses in the current study, while others involved modifications of the functional forms of the models. Development of the form of the model was performed for the larger horizontal component, with the same form assumed in the regressions for the model for the geometric mean of the orthogonal components. All statistical analysis was performed for the 11 periods up to 2.0s only, with the values for 3.0s added in the final stages.

Two simplifications have been made to the Abrahamson and Silva model for crustal earthquakes.

The Abrahamson & Silva large-magnitude value of the coefficient of the linear magnitude term for crustal earthquakes is used for all magnitudes, with the elimination of the small-magnitude coefficient. This resulted in improvements of the log-likelihood (*LL*) measures-of-fit for 7 of the 11 periods, even though the number of coefficients had been reduced, and better fits for all periods in terms of the Akaike Information Criterion (*AIC*) when the reduced number of coefficients was taken into account. It also overcame a problem with magnitude-dependence of the residuals of the New Zealand data that appeared to require the introduction of an additional coefficient for a magnitude-ln(distance) term for small magnitudes if separate values of the linear magnitude term were retained for small and large magnitudes.

The model uses Abrahamson & Silva's large-magnitude values of the period-dependent reverse/oblique style-of-faulting coefficients for all magnitudes. The elimination of the small-magnitude coefficients resulted in improvements of the *LL* measures-of-fit for 9 of the 11 periods considered, while the *AIC* value, accounting for one fewer parameter, indicated an improvement for all periods. The need for the small-magnitude coefficient in the Abrahamson & Silva model was marginal, in that it was largely controlled by the 1983 Coalinga aftershock sequence. This sequence contributed 8 of the 11 reverse and reverse/oblique events in the magnitude range less than 5.8 for which the small-magnitude coefficient applied. It is not included among the supplementary overseas data used in this study.

There are also four additions to the Abrahamson & Silva model, to extend its applicability in New Zealand.

An anelastic attenuation term, $C_5(T)r$, has been added for crustal earthquakes to extend the distance range of applicability of the model from 250 km to 400 km. The

increased distance range was required to obtain sufficient rock records and volcanic path records. Abrahamson & Silva used data for distances to about 250 km, for which the effect of anelastic attenuation is relatively unimportant.

A normal-faulting term for crustal earthquakes, corresponding to coefficient C_{32}, has been added to produce reduced estimates of the motions for earthquakes with normal-faulting mechanisms. Abrahamson (pers. comm.) found that normal-mechanism earthquakes from extensional regimes produce lower ground motions than strike-slip events from compressive regimes, in line with the results of Spudich *et al.* (1996, 1999), and provided the normal-mechanism term of -0.2 for *lnSA*, corresponding to a factor of 0.82 for *SA*, as a representative result. Although there is a reasonable representation of normal-faulting crustal earthquakes in the New Zealand dataset, with 7 normal events from the total of 24 crustal earthquakes, the coefficient C_{32} was not treated as a free parameter in the regression analysis because of shortcomings in the distribution of data from earthquakes with normal-faulting mechanisms. Only three of the normal-mechanism events produced more than one record suitable for use in the regression analyses. Fifty-one of the 62 New Zealand normal-faulting records came from the pair of earthquakes off East Cape in February 1995, all at distances exceeding 170 km from the source.

Greater attenuation in the Taupo Volcanic Zone (TVZ) of the North Island of New Zealand has been modelled by the additional anelastic attenuation term $C_{46}(T)\ r_{VOL}$ applied for crustal, shallow-slab and interface earthquakes, where the source-to-site path includes a distance r_{VOL} through the volcanic zone. Volcanic-path attenuation, including definition of the region over which it applies, is discussed in more detail in Section 9.1.

The number of site classes for which separate attenuation expressions were developed from the regression analysis was extended from two to three, as defined in Section 4. The site class terms are discussed in Section 8.

There are also modifications in the form of the Youngs *et al.* model for subduction zone earthquakes, as discussed in the following.

The single value for all periods of the coefficient C_{12Y} of the linear-magnitude term has been replaced by period-dependent coefficients $C_{12}^{*}(T)$, with associated changes in the coefficients $C_{17}(T)$ of the ln(distance term). The coefficients of these two terms linked through the $r=0$ near-source constraint that the magnitude-dependence is the same as for the Youngs *et al.* (1997) model at r=0, as given earlier in equation (7). Although the changes in the coefficient of the ln(distance) term $C_{17}(T)$ are statistically significant, all of the changes and the associated changes in the magnitude coefficients are small.

The depth coefficient $C_{20}(T)$ is a function of period, rather than being a constant value for all periods as in the Youngs *et al.* model. The depth coefficient for all periods except 3s is greater than the Youngs *et al.* value of 0.00607 km^{-1}, for example over double for pga with a value of 0.01550 km^{-1}. At 3s, the depth coefficient is negative. Crouse *et al.* (1988) found that their depth coefficients changed from positive at short periods, to near zero for periods of about 0.8s to 2s, and to negative for long spectral periods.

Differences between slab and interface earthquakes are modelled with an additive period-dependent term $C_{24}(T)$ for interface earthquakes, rather than by a period-independent value as in the Youngs *et al.* model. The pga value is similar to that of Youngs *et al.*, but over the period range of 0.1s to 0.3s is much larger. In the 0.75s to 2s range, the one standard error range suggests that the term is not statistically significant, with the error range spanning zero.

Volcanic path terms were introduced for interface and shallow slab earthquakes, through the same modification term as for crustal earthquakes. Similar effects occur at depth (e.g. Mooney, 1970), but in the current study these effects have been ignored for deep-slab earthquakes because of the difficulties of modelling the high attenuation zone in three dimensions. This aspect has been modelled by Eberhart-

Phillips and McVerry (2003).

Site effects are treated differently than in the Youngs *et al.* model. That model has separate expressions for rock sites and deep soil sites. In our model, three site classes are included through site-effect terms that are in common with those adopted for crustal earthquakes, as discussed in Section 8.

In addition, the following changes to the subduction zone expressions were considered, but rejected.

An anelastic attenuation term $\mathbf{C}_{14}(T)r$ was considered for subduction earthquakes, but was found to be statistically insignificant for the dataset containing source-to-site distances up to 400 km. The deep-slab subduction zone records used in the regression analyses are all for low-loss paths up the subduction slab, with the few records available for high-loss mantle paths excluded from the analysis. Anelastic attenuation in the subducting slab is much lower than for crustal paths.

The possibilities of different magnitude-dependence and attenuation rates for interface and slab earthquakes were investigated, but the extra parameters required to improve the fit were not justified in terms of the *AIC*. This is at odds with the recent results of Atkinson & Boore (2003), who found less rapid attenuation for interface earthquakes. They also found that the interface geometric attenuation rates are strongly magnitude-dependent, with the attenuation rates decreasing for larger magnitudes. The lack of stronger magnitude dependence for interface earthquakes in the New Zealand database may reflect insufficient data from large-magnitude interface earthquakes (see Section 10.4).

Different depth dependence for interface and slab earthquakes was investigated, but the extra parameters required to improve the fit were not justified in terms of the AIC.

The possibility of an additive deep slab term $C_{47}(T)$ was considered, but the standard error bounds showed that this was significantly different from zero only for T=0.075s, and not significant by the *AIC* for any period.

8. SITE EFFECT TERMS

Site effects are modelled by soil response factors that may be nonlinear functions of rock pgas, as in the Abrahamson & Silva model, to represent nonlinear soil response in earthquakes.

The functional form is similar to the simple nonlinear hyperbolic stress-strain relation used in geomechanics for the strain-dependent shear modulus $G(\gamma)$

$$G(\gamma) = G_0 / (1 + |\gamma / \gamma_{ref}|) \qquad (10)$$

In an analogous manner, the site effect expression for class D can be rewritten as

$$AMP_D(T) = SA_D(T)/SA_{rock}(T) = AMP_D(T, PGA_{rock}=0) / (1 + PGA_{rock}/PGA_{ref})^p \qquad (11)$$

with

$$AMP_D(T, PGA_{rock}=0) = \exp(C_{43}(T)) / (PGA_{ref})^p \qquad (12)$$

$$PGA_{ref} = 0.03g \qquad (13)$$

$$p = -C_{30}(T) \qquad (14)$$

where $AMP_D(T)$ is the amplification of the Class D spectrum with respect to the rock spectrum, and the exponent p is positive for periods less than 1s.

A feature to note about the nonlinear soil term is that the amplification is a function of the predicted *median* rock pga, rather than the rock pga for the same probability of exceedance level as for the soil response being considered. Thus the predicted amplification at a soil site for the 84-percentile spectrum for some magnitude and distance with respect to the 84-percentile rock spectrum is the same as for

the median soil spectrum with respect to the median rock spectrum, even though the 84-percentile rock pga may be 50% or more greater than the corresponding median value. This feature requires a constant amplification for a particular earthquake and site combination independent of the percentile levels of the motion being considered, while the model is intended to represent nonlinear amplification. Conversely, the amplification for a closer or larger magnitude earthquake will be less for the same rock acceleration, because its median acceleration will be greater. This second situation is more plausible, at least for the larger magnitude earthquake, in that nonlinearity may be a function of duration of shaking, which is generally longer for a larger magnitude earthquake for the same source-to-site distance, as well as the amplitude of the motion.

Another feature of the Abrahamson & Silva-type nonlinear site response term is that at long spectral periods the amplification increases rather than decreases with rock pga. The changeover occurs at 1s period, for which the response is linear i.e. the amplification is constant for all rock pga values. This facet of the model simulates the feature of results of nonlinear soil response modelling that there is a transfer of energy from high frequencies (short periods) in the input rock motions to low frequencies (long periods) in the soil response. The long-period soil response is partly excited by shorter-period rock motions, while for linear response it would be directly related to the input rock motion at the same spectral period. Highly nonlinear response may actually attenuate the short-period motions with respect to the rock motions, with some of the energy appearing as long-period soil motions, thus producing an increasing amplification with increasing rock pga in the long-period band. However, the soil response term in the Abrahamson & Silva model only departs slightly from a linear amplification expression at long periods, while allowing a significant reduction of the amplification, or even attenuation, at short periods.

In this study, the linear site response parameters $C_{29}(T)$ and $C_{43}(T)$ were free coefficients in the regression analyses. Obtaining the coefficients of the nonlinear site response terms was more difficult, with free regressions producing unacceptable (positive) values of the coefficient of this term for short periods for site class C (Shallow Soil Sites). Constraint to negative values produced poorer fits than obtained with a linear site response term, which was the final selection for this site class. For Class D (Deep or Soft Soil Sites), constraint to the Abrahamson & Silva values gave a slightly improved fit than a linear term according to the Log Likelihood. The Abrahamson & Silva coefficients were accepted for Class D to allow nonlinear response even though the extra term was not justified in terms of the AIC. The inability to justify the nonlinear terms statistically may well be because of insufficient strong records in the New Zealand dataset, given the lack of near-source records.

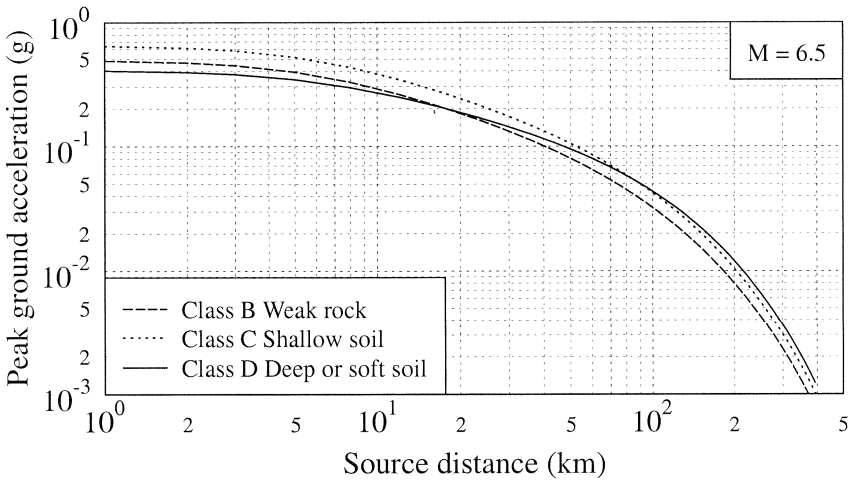

Figure 8: Pga attenuation curves for the three site classes for a magnitude 6.5 reverse-mechanism earthquake.

Figure 8 shows the effects of site class on pga attenuation curves for a magnitude 6.5 reverse-mechanism earthquake. At short distances where rock pgas are about 0.2g and greater, pgas are strongest for Class C shallow soil, followed by Class A/B rock and Class D deep or soft soil, with values at 1 km from the source of 0.64g, 0.48g and 0.40g respectively. The Class D pgas are affected by nonlinear soil response, being stronger than the rock pgas at values of about 0.2g and less, and stronger than the Class C pgas below about 0.05g.

Similar behaviour for response spectra is demonstrated in Figures 9a and 9b, for reverse-mechanism earthquakes of magnitude 6.5 at a distance of 20 km and of magnitude 5.5 at 50 km from the source. The ordering of the spectral accelerations for the three site classes are both period-dependent and amplitude-dependent. At long periods, the deep or soft soil values are greatest, followed by shallow soil and rock. At short periods, the shallow soil values remain stronger than the rock values, but the deep or soft soil values may lie anywhere from strongest at low pga values to weakest for strong pgas. For the magnitude 6.5 earthquake at a distance of 20 km, corresponding to a rock pga of 0.18g, the short-period part of the spectrum for deep or soft soil for periods up to about 0.2s is similar to the rock spectrum. At longer periods, the deep soil spectrum becomes increasingly amplified with respect to the rock spectrum, becoming stronger than the shallow soil spectrum for periods in excess of about 0.5s. For the weaker motions (about 0.048g rock pga) from the smaller magnitude 5.5 earthquake at the greater distance of 50 km, the deep or soft soil spectrum is stronger than the rock spectrum for all periods. It is similar to the shallow soil spectrum for periods up to about 0.4s, before becoming considerably stronger than the shallow soil spectrum at long periods.

An unexpected feature is that the shallow soil and rock spectra are similar at long periods, for 1.5s and greater. This behaviour is likely to be spurious, indicating a deficiency of data at longer spectral periods.

9. REGIONAL ATTENUATION EFFECTS

Regional attenuation has been considered for three situations in this study, namely for crustal attenuation in the Taupo Volcanic Zone (TVZ), for attenuation in the mantle wedge above part of the Hikurangi subduction zone, and for the Fiordland subduction zone. Crustal attenuation in the TVZ is accounted for by a volcanic-path term in the model, as discussed in Section 9.1. Mantle attenuation effects are the subject of a paper by Eberhart-Phillips & McVerry (2003). Possible differences in the Fiordland subduction zone are not accounted for in the model, but the issues are discussed in Section 10.4 that compares the model predictions with recorded motions in Fiordland interface earthquakes, particularly the magnitude 7.2 earthquake of 21 August 2003 and its aftershocks.

9.1 Crustal Attenuation in the Taupo Volcanic Zone

High attenuation of earthquake waves in the volcanic region of the North Island has been recognised for many years, both at depth (e.g. Mooney, 1970) and in the crust (e.g. Haines, 1981). Seismograph records show that the increased attenuation in the volcanic region has much less effect at low frequencies than at high frequencies. Our model quantifies the increased attenuation in the volcanic region for response spectral accelerations at a range of periods from 0s (corresponding to pga) to 3s. The model presented in this paper accounts for increased attenuation in the crustal part of the volcanic zone. The high attenuation zone at depth in the mantle wedge under the volcanic zone above the subducting Pacific Plate, which is estimated to reduce spectra by factors of approximately 2-4 (Eberhart-Phillips & McVerry, 2003), is not represented by the model in this paper.

One aspect of the volcanic path study was defining the region over which the volcanic path term applies. Cousins *et al.* (1999) considered several possibilities for the geographic extent of the highly attenuating part of the volcanic region. They considered the "CVR (Central Volcanic Region)", "whole TVZ (Taupo Volcanic Zone)" and "young TVZ", as defined by Wilson *et al.* (1995) and shown in Figure 10.

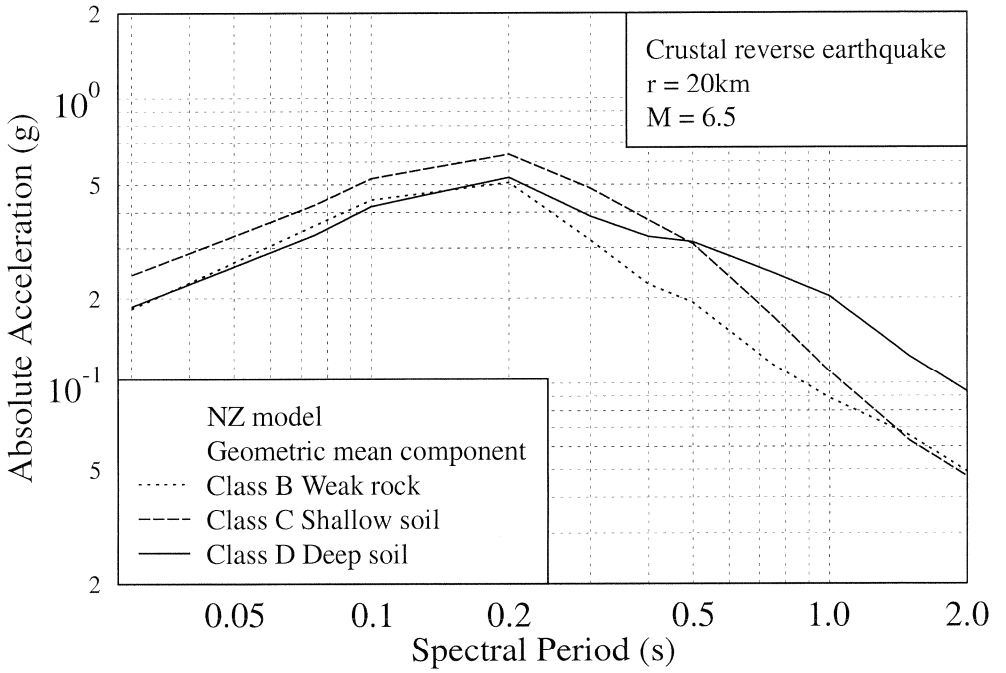

(a)

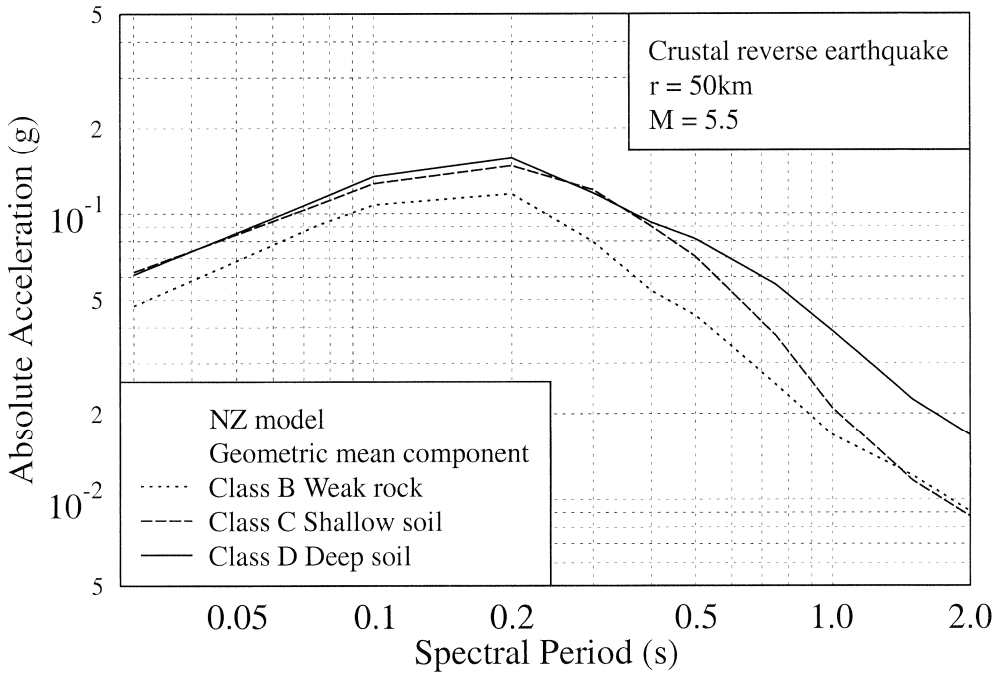

(b)

Figure 9: Effect of site class on spectra for (a) magnitude 6.5 reverse-mechanism earthquake at 20 km and (b) magnitude 5.5 reverse-mechanism earthquake at 50 km. Note the different order of the spectra for the three site classes depending on spectral period and rock pga values.

From analysis of residuals of pgas estimated using a model developed for non-volcanic paths, Cousins *et al.* deduced that the "whole TVZ" appeared the best representation of the three candidates considered for the highly attenuating crustal volcanic zone. We have followed Cousins *et al.* in adopting the whole TVZ of Wilson *et al.* as the highly attenuating zone in this study. Dowrick and Rhoades (1999) found a very similar region of high attenuation in a study of Modified Mercalli intensities.

The whole TVZ is much smaller in extent than the simplified CVR region defined by Haines (1981) for special treatment in the determination of local magnitudes, M_L. Haines' CVR was not considered as one of the candidates for the high attenuation region by Cousins *et al.* It appears that it would be a less satisfactory choice than the whole TVZ for modelling the data of our study, in that it includes some of those areas demonstrated by Cousins *et al.* as having attenuation similar to the rest of the country.

Total residuals (i.e. data minus predicted values) for *lnSA* are shown for the pga data involving volcanic paths in Figure 11 for a model with no volcanic path term. Figure 12 is for a model of the same type but including the volcanic path term in the regression.

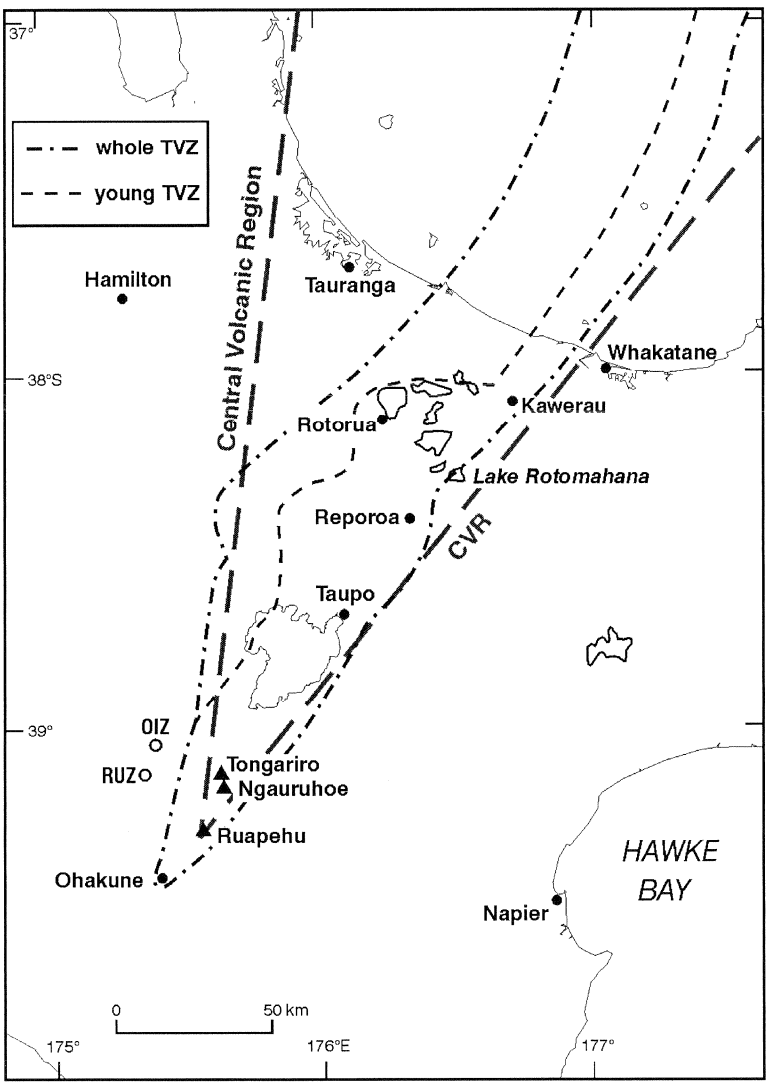

Figure 10: The Central Volcanic Region (CVR), whole Taupo Volcanic Zone (TVZ) and young TVZ considered as candidates for the highly attenuating volcanic region by Cousins et al. (1999). The whole TVZ has been selected as the highly attenuating region in this study, as suggested by their results. Figure adapted from Wilson et al. (1995).

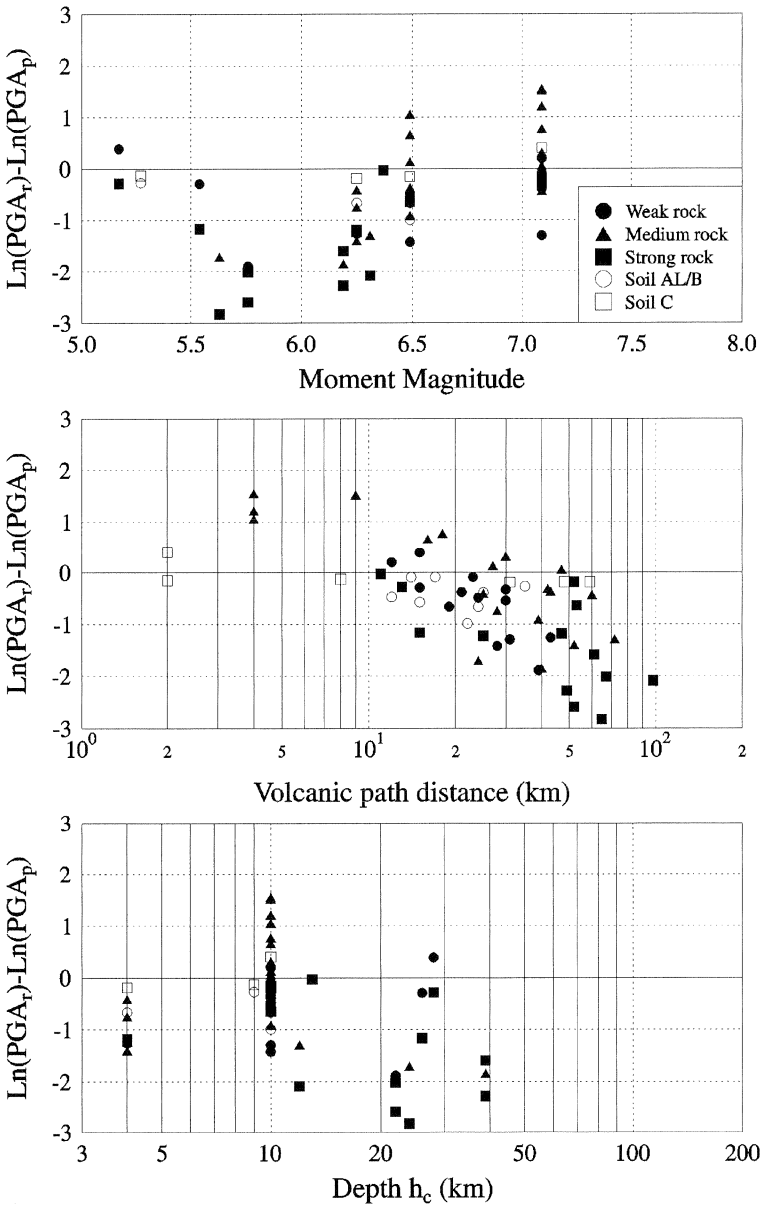

Figure 11: Residuals for volcanic path data, for a model with no volcanic path term. Note the poor fits, and the strong trend of increasingly negative residuals (i.e. the model over-predicting the data) with volcanic path distance.

Plots of the residuals as a function of magnitude, volcanic path distance and depth in Figures 11a-c all show evidence of poor fits for the volcanic path data. Particularly apparent is a trend of residuals becoming increasingly negative (i.e. increasingly over-estimated) as the volcanic path distance increases. Figure 12, including the volcanic path term, shows that this trend has been removed. Note that these plots are not for the final model, as changes to other aspects of the model were made subsequently, but demonstrates the effectiveness of the addition of the volcanic path term at the stage that it was added during model development.

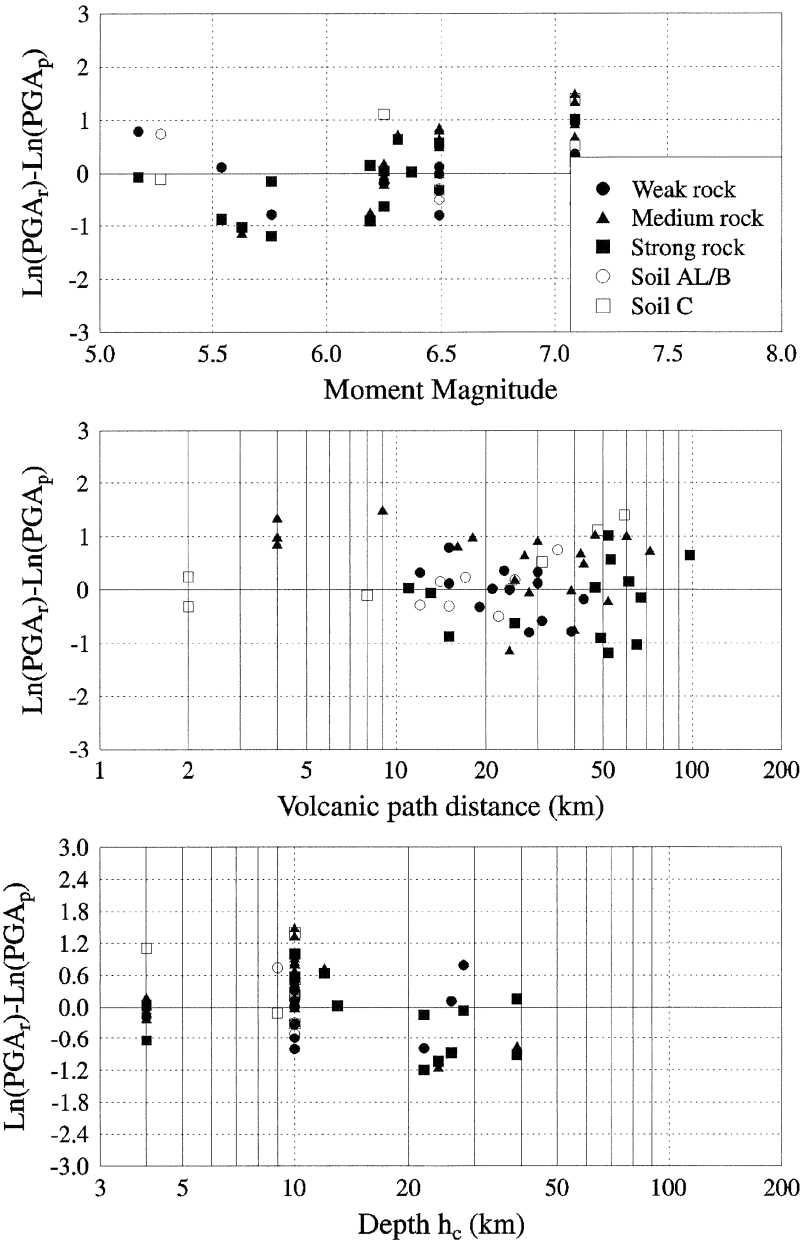

Figure 12: Residuals for volcanic path data, for the model of Figure 11 modified to include a volcanic path term. Note the much improved residuals, and the removal of the trend with volcanic path distance.

Values of the period-dependent coefficient $C_{46}(T)$ of the volcanic path term are listed with the other coefficients of the attenuation models in Tables 5 and 6. The volcanic path coefficients are in the range -0.032 km^{-1} to -0.039 km^{-1} for periods up to 0.5s, before gradually reducing in size to -0.017 km^{-1} at T= 3.0s. Cousins *et al.* (1999) found a value of -0.031 km^{-1} for pga, using a similar dataset but considerably different form of attenuation model. For our model, the volcanic path attenuation coefficients range between 3.4 and 4.4 times the values for crustal earthquakes in the non-volcanic region in the period range 0s to 1s. For records from sites with paths entirely within the volcanic region, this means that the total anelastic attenuation term (for *lnSA*) ranges between 4.4 and 5.4 times that for totally non-volcanic paths of the same length. While the geometric attenuation (i.e. ln distance) term provides most of the reduction in ground motions with distance for non-volcanic paths at distances less than 100-200 km, the geometric and anelastic attenuation are of similar importance for volcanic paths for even short distances. The total anelastic attenuation term halves pga values over only 16 km in the volcanic region, while requiring more than 70 km to have the same effect on its own (i.e. neglecting the geometric attenuation) outside the volcanic zone. Pga attenuation curves for volcanic and nonvolcanic paths are shown in Figure 13. The volcanic path effect is less severe for periods exceeding 0.5s.

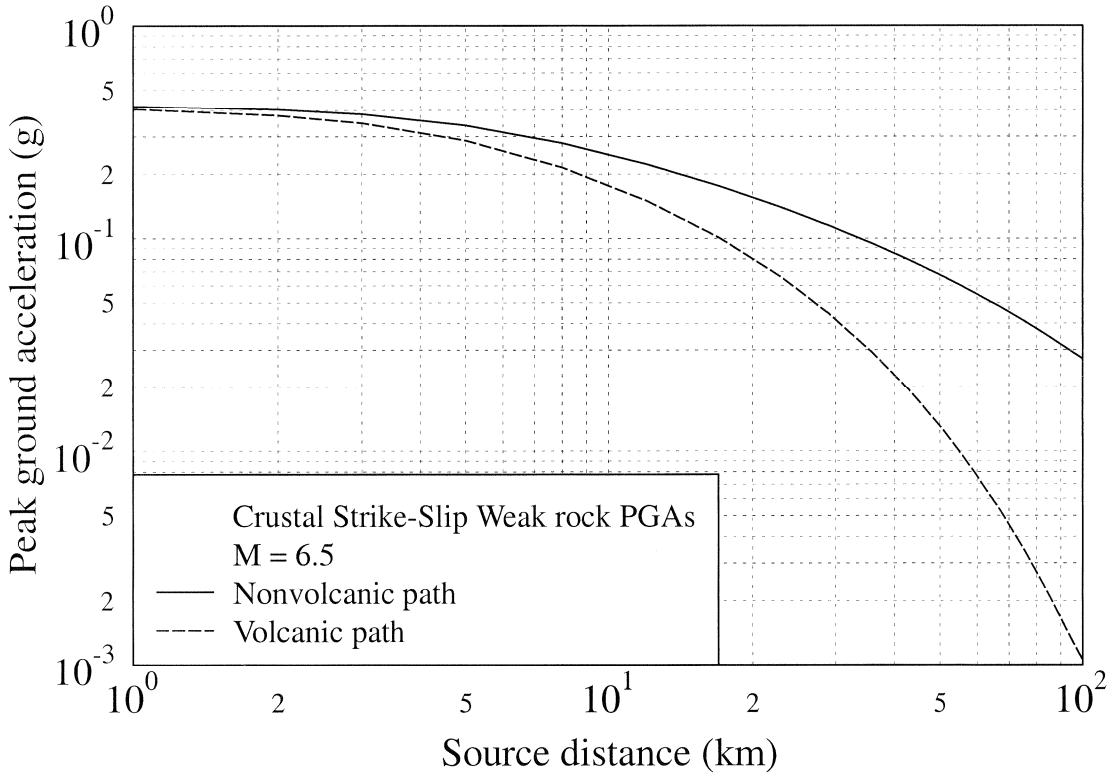

Figure 13: Plot demonstrating the very rapid attenuation of pga for paths completely within the "whole TVZ" volcanic region compared to that for non-volcanic paths, for the final model.

10. EXAMPLES OF PREDICTED SPECTRA

This section compares the spectra and attenuation curves for the New Zealand attenuation model developed in this study with those of the Abrahamson & Silva (1997) and Youngs *et al.* (1997) models from which it has been modified, and compares pga attenuation curves with those of the earlier Zhao *et al.* (1997) pga model for New Zealand. It also demonstrates the differences in spectra for different tectonic types of earthquakes, and for different mechanisms for

crustal earthquakes. Site effects were demonstrated in Section 8.

10.1 Comparison with Abrahamson & Silva model for crustal earthquakes

Figure 14 compares spectra of the New Zealand and Abrahamson & Silva model for deep soil sites for a magnitude of 7.5 at distances of 3 km, 10 km and 30 km for reverse-mechanism earthquakes. The comparisons are in terms of the geometric mean spectra of the two components, as used in the Abrahamson & Silva model. The Abrahamson & Silva model gives considerably higher pgas at short distances, but attenuates more rapidly with distance at all spectral periods. Unlike those of the Abrahamson & Silva model, the coefficients of the New Zealand model have not been smoothed as a function of period. The lack of smoothing is reflected in the spectra, especially at shorter distances.

Figure 15 shows a similar comparison of the Abrahamson & Silva rock spectra with the New Zealand rock spectra and shallow soil spectra. The Abrahamson & Silva rock class overlaps the New Zealand rock and shallow soil classes, and this is apparent to some extent in the spectra. Crustal spectra for the New Zealand Shallow Soil class are generally similar to the "rock" spectra of Abrahamson and Silva, and those of the Deep Soil class to their "soil" spectra. Crustal weak-rock spectra are generally weaker than those of Abrahamson & Silva, apparently because of the combination of rock and shallow soil sites in the Abrahamson & Silva "rock" class.

The comparison of the spectra for the New Zealand site classes with the "rock" and "soil" site classes are in line with discussion of the Abrahamson & Silva rock and soil classes by Rodríguez-Marek, Bray and Abrahamson (2001). They note that the spectra for Abrahamson & Silva rock sites in the Northridge earthquake were generally similar to those for "shallow and intermediate depth soils and weathered/soft rock", with the spectra for competent rock sites approximately 30% lower on average. They further stated that "this result reflects the fact that for the joint database of rock and shallow soil sites, 83% of the sites are shallow soil or weathered rock sites, and only 17% of these sites actually belong to...competent rock sites." They also found that the spectra for Abrahamson & Silva soil classes were representative of those for deep soil sites (soil depths greater than 60 m).

The reasons for the New Zealand model giving weaker pgas than the Abrahamson & Silva model at short distances for all soil classes is unknown. Preliminary results of the PEER Next Generation Attenuation (NGA) project in California indicate that near-source accelerations from the Abrahamson & Silva model have been considerably reduced in the new models (M. Stirling, pers. comm.).

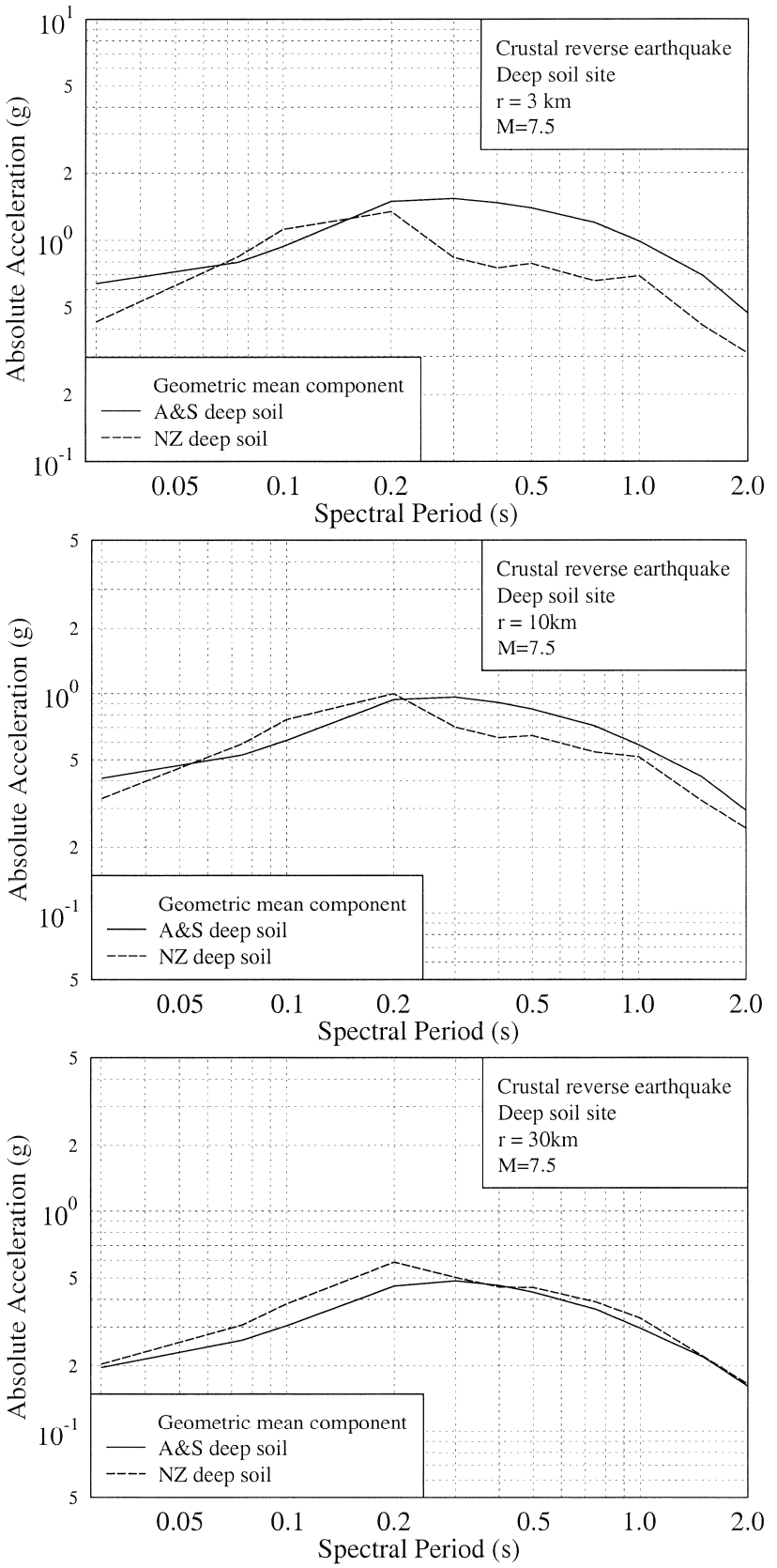

Figure 14: Abrahamson & Silva soil spectra and New Zealand deep soil spectra for magnitude 7.5 reverse mechanism earthquake at distances of 3, 10 and 30 km.

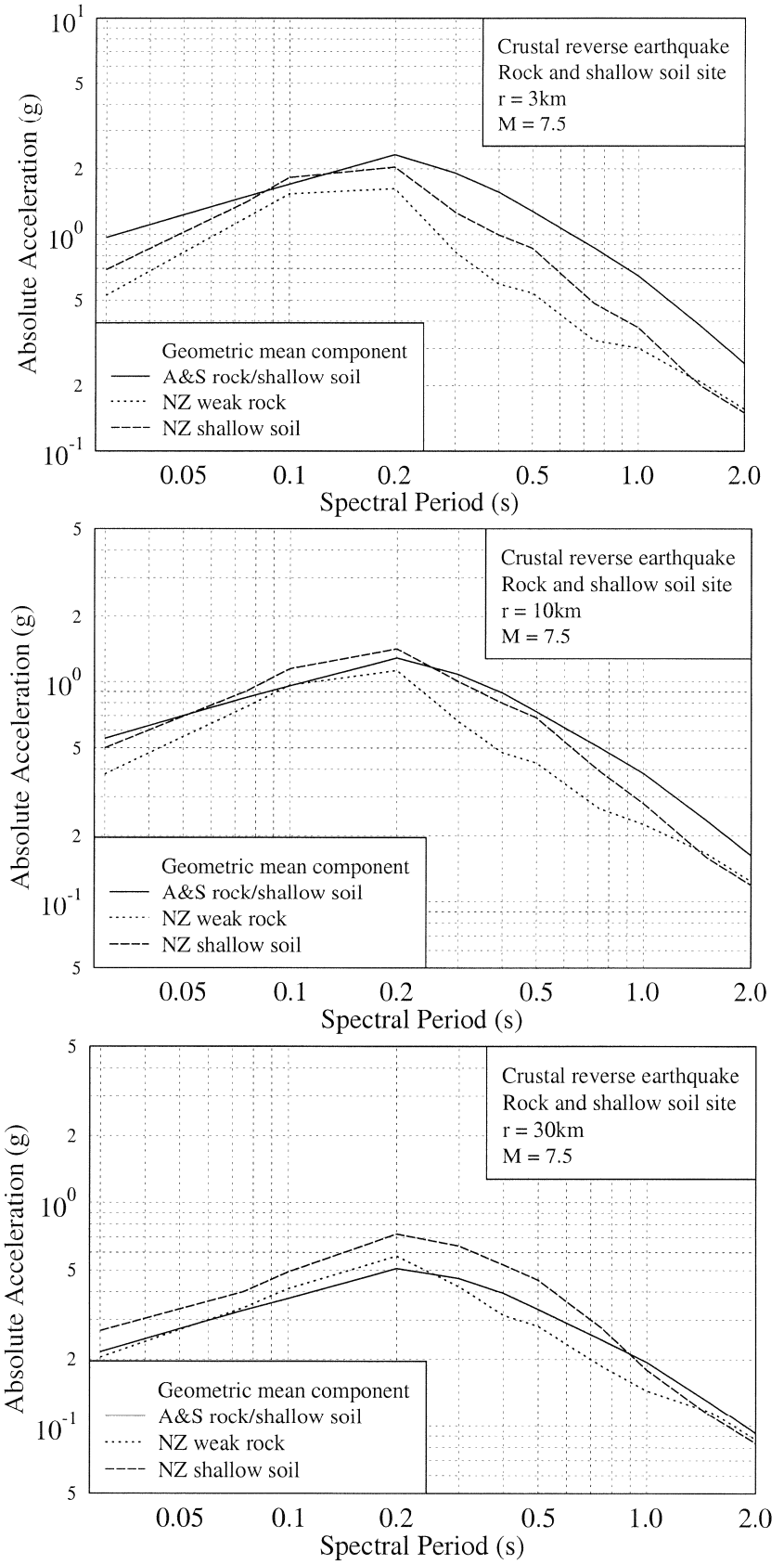

Figure 15: Abrahamson & Silva rock spectra and New Zealand rock spectra and shallow soil spectra for a magnitude 7.5 reverse crustal earthquake at distances of 3, 10 and 30 km.

10.2 Comparison with Zhao *et al.* (1997) New Zealand pga model

This study used the pga dataset of the Zhao *et al.* (1997), apart from the exclusion of records from very soft soil sites and from the basements of buildings greater than four storeys in height, supplemented by digital seismograph records. The crustal and subduction zone models developed in this study had different functional forms from the Zhao *et al.* model. The Zhao *et al.* model was of the Boore-Joyner-Fumal type, with no magnitude saturation. Also, crustal and subduction earthquakes shared the same expression, apart from a reverse-mechanism term for crustal reverse earthquakes and an interface term for subduction interface terms. The Zhao et al. model has identical expressions for crustal earthquakes with normal or strike-slip mechanisms and subduction slab earthquakes with the same centroid depth. The Zhao *et al.* model also combines site Classes C, D and E into a single soil class.

Peak ground acceleration curves for site class C (Shallow Soil) and the Zhao *et al.* soil class are compared in Figure 16 for reverse mechanism crustal earthquakes with centroid depth of 10 km, and in Figure 17 for subduction slab earthquakes with a centroid depth of 20 km. The comparisons are shown for magnitudes of 5.5, 6.5 and 7.5. The plots are shown for the larger horizontal component, consistent with the definition of the Zhao *et al.* model.

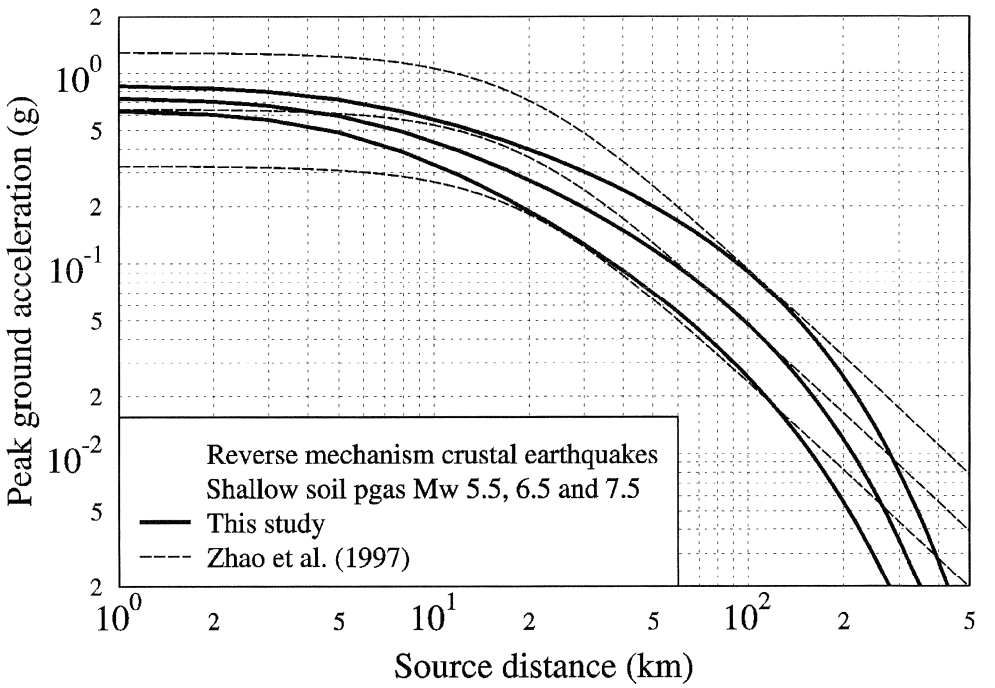

Figure 16: Comparison of pga attenuation curves for reverse mechanism crustal earthquakes for the shallow soil site class of this study and the soil class of Zhao et al. (1997). The plots are for the larger horizontal component.

The attenuation curves for reverse-mechanism crustal earthquakes are very similar for the two models for all magnitudes for distances of about 80 km to 150 km. At shorter distances, the magnitude-saturation feature of the current model causes the three curves to be much more closely spaced than for the Zhao *et al.* model. The near-source pga of about 1.3g at magnitude 7.5 for the Zhao *et al.* model appears rather high, but equally its near-source estimate of about 0.3g for a magnitude 5.5 earthquake may be more realistic than about 0.6g in the current model. At

distances greater than 150 km, the inclusion of an anelastic attenuation term in the current model produces more rapid attenuation than for the Zhao *et al.* model.

Comparisons for rock and strike-slip or normal mechanism earthquakes show greater discrepancies, in that the values of various factors are different in the two models. The Zhao *et al.* reverse fault factor of 1.48 and soil class factor of 1.54 are both considerably larger than the values of 1.30 and 1.35 in the current model. The Zhao *et al.* magnitude-independent standard deviation for *ln(pga)* of 0.53 is intermediate between the values of 0.45 for magnitudes of 5.0 and less and 0.67 for magnitudes of 7.0 and greater in the current model.

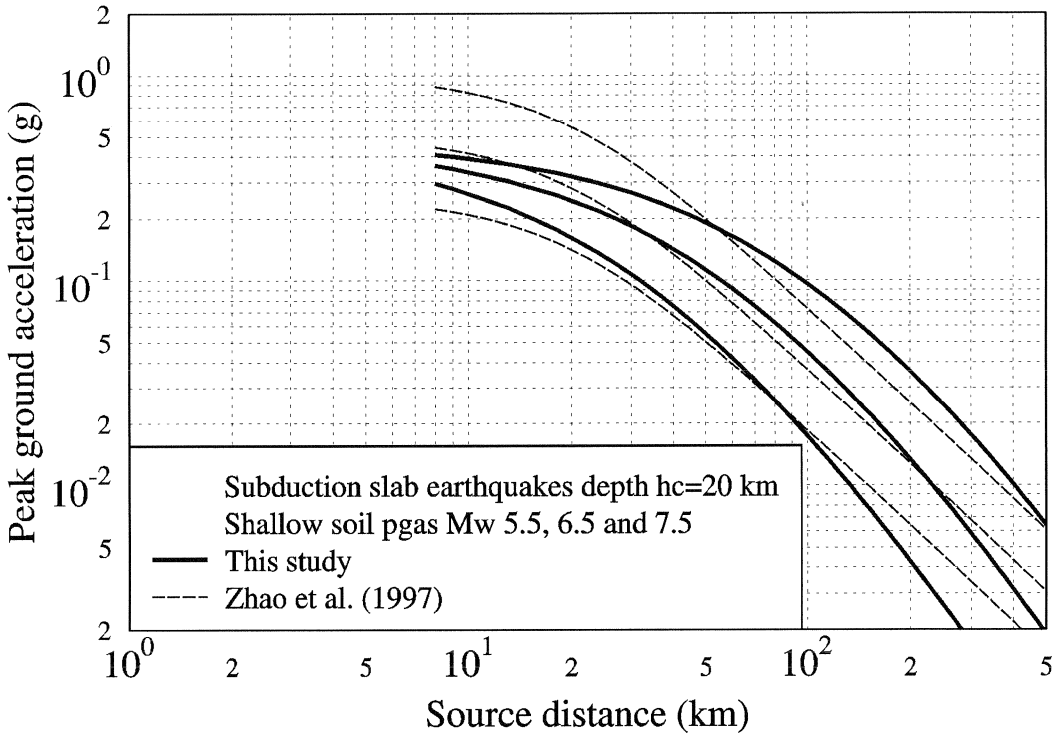

Figure 17: Comparison of pga attenuation curves for shallow subduction slab earthquakes with centroid depths of 20 km for the shallow soil site class of this study and the soil class of Zhao et al. (1997). The plots are for the larger horizontal component.

For shallow subduction slab earthquakes, the pga values for magnitude 6.5 are generally similar for the Zhao *et al.* and the current model for distances of about 20 km to 300 km, but the shapes of the attenuation curves and their magnitude-dependence are different (Figure 17). Magnitude-saturation is apparent in the current model at short distances. A maximum 50-percentile pga of about 0.4g at magnitude 7.5 rather than about 0.9g as in the Zhao *et al.* model appears more realistic. The scaling with magnitude is greater for the current model than for Zhao *et al.* at large distances. The attenuation rate is considerably greater for the current model at large distances.

The dependence on centroid depth is similar for the two models, with a coefficient of 0.0155 km^{-1} for the current model compared with 0.0140 km^{-1} in the Zhao *et al.* model for *ln(pga)*. There are greater differences between interface and slab pgas in the current model, with a factor of 0.60 in the current model compared to 0.75 in the Zhao *et al.* model.

10.3 Comparison of crustal, interface and slab motions

The different characteristics of crustal, interface and shallow-slab spectra are indicated in Figure 18, for the shallow soil site class at a source-to-site distance of 30 km and a magnitude of 7.0, with a centroid depth of 20 km. All three

spectra are similar for periods beyond 0.75s, but the interface spectrum is considerably weaker at short periods. The reverse-faulting crustal event has the strongest pga of the three spectra, but the spectral peak at 0.2s is strongest for the shallow slab event. The interface and shallow slab spectra retain the same ratio to each other for all magnitudes, but for lower magnitudes, the reverse crustal and shallow slab spectra are similar to each other for periods of 0.2s and longer, while the crustal spectrum is stronger at shorter periods down to 0s (pga).

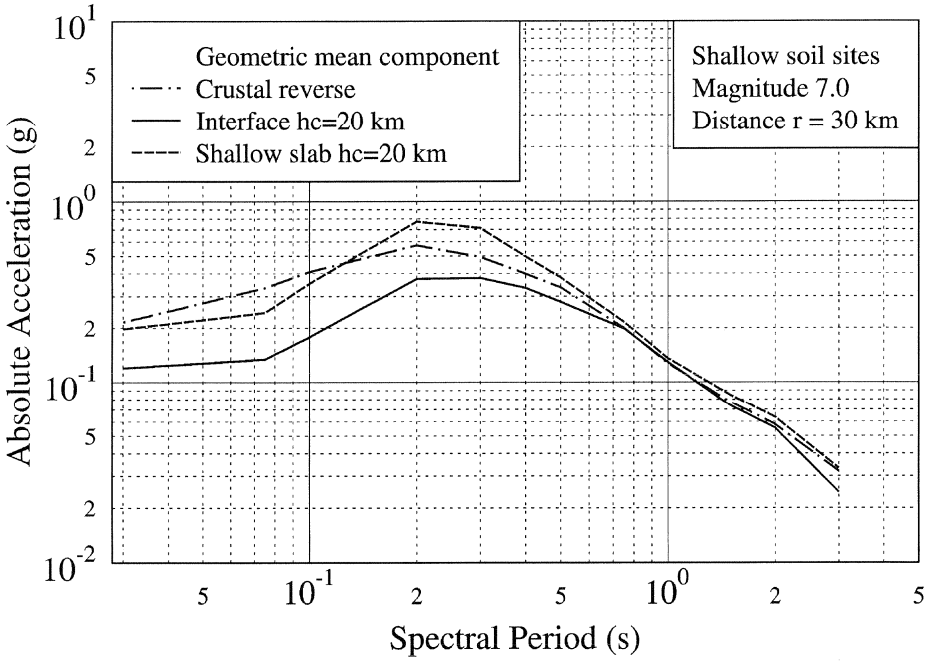

Figure 18: Comparison of spectra of crustal reverse, and subduction zone interface and shallow slab events at a distance of 30 km from the source. The subduction zone events are at centroid depths h_c of 20 km

This comparison is one illustration of the potential problems that could arise from relying on mechanism alone to distinguish types of earthquake, taking no account of different tectonic classes of earthquakes, because the motions for crustal earthquakes vary differently with mechanism than those for subduction zone earthquakes. For crustal earthquakes, we found that reverse mechanism events produce the strongest motions, followed by strike-slip and normal events. However, for subduction zone events, the reverse mechanism interface events have the lowest motions, at least in the period range up to about 1s and distances less than about 100 km, while the slab events, usually with normal mechanisms, are generally strongest, a finding that is in agreement with the results of Youngs *et al.* (1997) and Atkinson and Boore (2003).

The modelled spectra for slab earthquakes appear overly peaked. For example, in Figure 18 the peak of the shallow slab spectrum is about 4 times the pga value, where values of 2.5 to 3 are more typical in other models. The peaked shape is most acute at large magnitudes where there are no data, with the greater attenuation rates than in the Youngs *et al.* model demanded by the New Zealand data also increasing the magnitude coefficient through the linking of these terms by the near-source constraint. A different constraint, of retaining the Youngs *et al.* magnitude coefficient but allowing the attenuation rate to be free in the regression, leads to spectra that appear unconservatively weak for large magnitudes.

A surprising feature of the model is that while the spectral shapes and pga values vary between the different tectonic

categories of earthquake, the attenuation rates appear similar except at large distances, as shown in Figure 19. The difference at large distances arises because the crustal earthquake model includes an anelastic attenuation term $C_5(T)r$ that is not required in the subduction earthquake expression. Plots of anelastic attenuation rate derived from inversions of the velocity and Q-structure in the slab and crust show that the anelastic attenuation rate in the slab is considerably less than in the crust (e.g. Eberhart-Phillips & McVerry (2003)), but this difference has little effect at distances less than about 150 km because geometric attenuation dominates out to this distance.

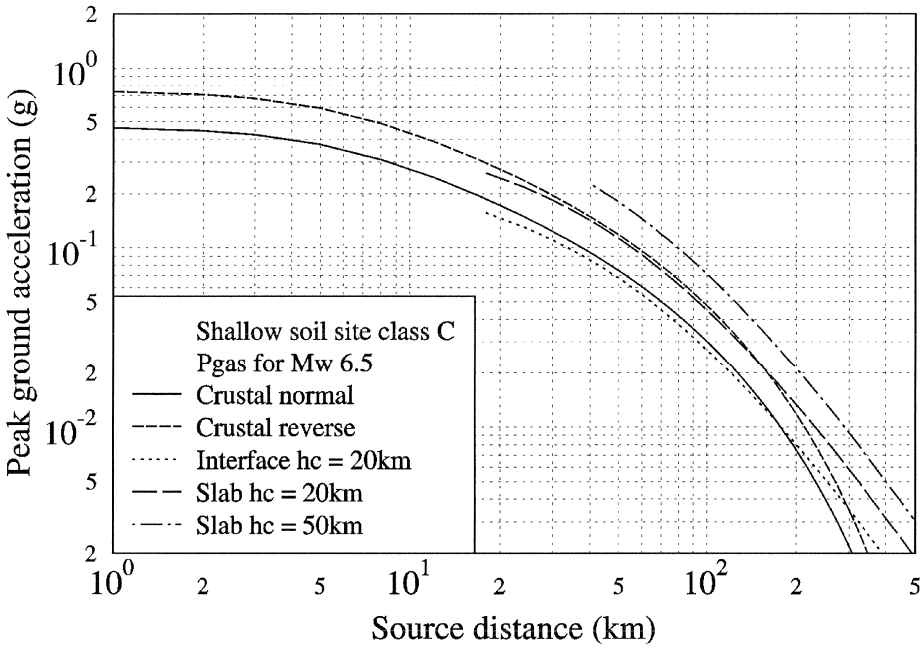

Figure 19: Comparison of pga attenuation curves for the stronger component for different mechanisms and tectonic categories. Depth has a marked effect on pga values. The attenuation rates are similar for crustal and subduction zone earthquakes for distances up to about 150 km, beyond which the reduced anelastic attenuation in the subducting slab has effect.

10.4 Comparison with motions in the M_W 7.2 Fiordland earthquake and its aftershocks

The possibility of ground motions in Fiordland earthquakes being different from those in other parts of the country has been discussed for many years. Haines (1981) gave a different attenuation expression for calculating local magnitude for Fiordland earthquakes. Smith (1978) found that intensities for Fiordland earthquakes for a given magnitude and distance are less than those for earthquakes elsewhere in the country, and adjusted his standard attenuation expression for Modified Mercalli intensities for Fiordland earthquakes.

In the current study, Fiordland earthquakes have been treated as having the same attenuation expressions as those of the same tectonic type occurring elsewhere in New Zealand. This issue can now be revisited, by comparing the predictions of the attenuation model with peak ground accelerations and acceleration response spectra from the M_W 7.2 Fiordland earthquake of 21 August 2003 and its aftershocks, as well as with the data from earlier Fiordland earthquakes that were used in developing the model. Overall, peak ground accelerations and spectra for New Zealand subduction interface earthquakes overall are matched well by the model.

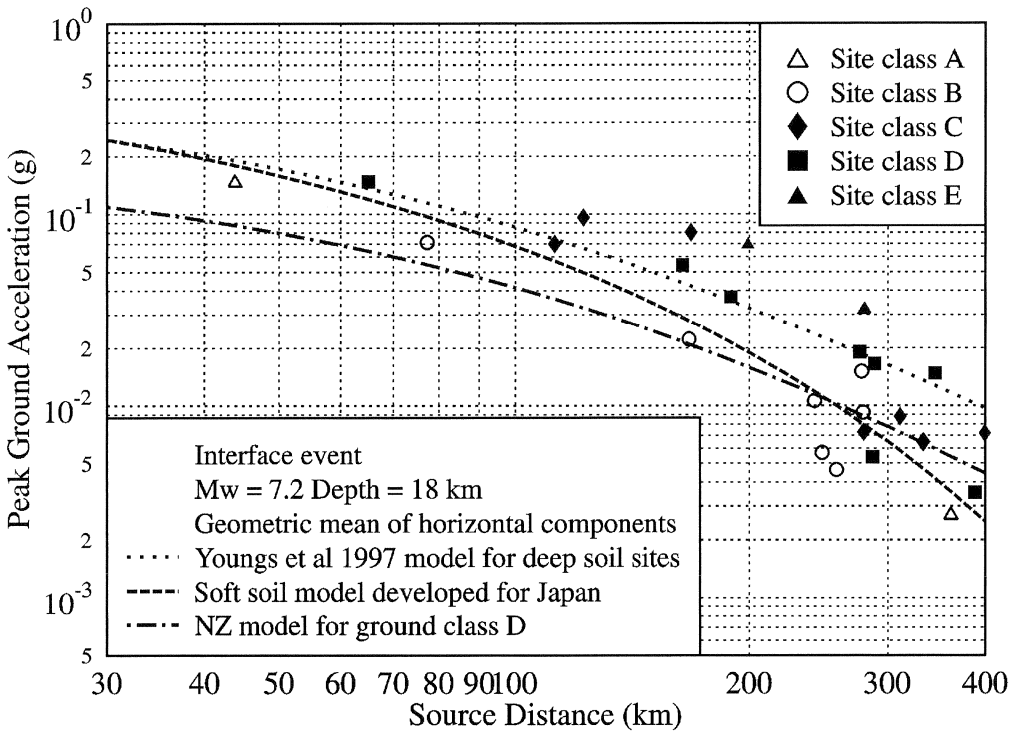

Figure 20: Comparison of the Fiordland mainshock pga data with three attenuation models for deep or soft soil conditions. The New Zealand model under-estimates the data by a factor of 1.6 on average.

Figure 20 compares the recorded pgas in the M_W 7.2 Fiordland subduction interface earthquake of 21 August 2003 with the New Zealand and two other attenuation models for subduction interface earthquakes. The plots are for the 50-percentile values of the geometric mean of the peak accelerations of the two horizontal components. The attenuation curves shown are for the site classes believed to be most appropriate for New Zealand deep or soft soil sites (excluding very soft soil sites), the most common classification for these records, although the appropriate New Zealand site class A to E is denoted for the individual records. The deep soil class gives the strongest peak ground accelerations for each of the models, and corresponds to the data plotted as solid squares.

The peak ground accelerations in the Fiordland mainshock were considerably under-estimated by our New Zealand model, by a factor of about 1.6 on average for pgas at distances up to 400 km when allowance is made for site conditions. The pgas were matched better by the Youngs *et al.* (1997) model that served as the starting point for the attenuation expressions developed for subduction zone earthquakes. The Saiki *et al.* (2003) model developed from Japanese data is intermediate between the Youngs *et al.* and New Zealand models. The attenuation curves of the New Zealand model for 5% damped response spectral accelerations for periods of 0.5s, 1s and 2s (not shown) also under-predict the values recorded in this earthquake.

Our New Zealand model has provided similar under-estimation of the motions in the only two previous Fiordland subduction interface earthquakes for which accelerations records have been obtained. The magnitude 6.4 Fiordland earthquake of 31 May 1989 was under-predicted by an average factor of 1.7, with a factor of 1.4 for the magnitude 6.8 Secretary Island earthquake of 10 August 1993. Under-prediction of motions in Fiordland interface earthquakes disagrees with the Fiordland adjustment factors of Smith

(1978), which suggest that motions in Fiordland earthquakes are usually less for a given magnitude and distance than elsewhere in New Zealand, but that model didn't differentiate between crustal, interface and shallow slab earthquakes. The data available for the 1978 study were very sparse and of low quality (Smith, pers. comm.).

The New Zealand model generally performed better for the Fiordland aftershock pga data (Figure 21) than for the mainshock. As most of the aftershock data, especially for distances up to 100 km, were from strong rock sites, the attenuation curves have been plotted for rock, rather than for deep or soft soil as in the mainshock. Unlike for the mainshock, the New Zealand model provides a better fit than the Youngs *et al.* model. For the smaller magnitude events (magnitude 5.0 and 5.1), all three attenuation relations generally over-predicted the data. For two magnitude 5.5 events, the New Zealand model gave a reasonable match to the rock pgas, while the other models tended to over-predict them. For the largest magnitude aftershock for which data is available (M6.1), the New Zealand model generally under-predicts the rock data, while the other two generally over-predict, apart from the strongest record with 0.28g pga obtained at 23 km hypocentral distance.

Thus the situation is not as simple as indicated by the mainshock, where it could be claimed that the Youngs *et al.* model was much better than the New Zealand model, which under-predicted the data. For the aftershocks, the New Zealand model was generally better than the Youngs *et al.* model.

A general observation is that the magnitude-dependence shown by the data was greater than that shown by any of the three models. This is demonstrated by the pgas from the mainshock generally being under-predicted, while those from the aftershocks around magnitude 5.0 were generally over-predicted.

The magnitude 7.2 earthquake and its aftershocks for which strong-motion data is available, spanning magnitudes 5.0 to 6.1, considerably expand the amount and magnitude range of data from New Zealand subduction interface earthquakes. Prior to this series of subduction interface earthquakes, the data included only 11 Fiordland interface records from two earthquakes, making it difficult to develop and statistically justify modification terms for Fiordland. The 2003 Fiordland earthquake provided a further 25 records for site classes A to D at distances of less than 400 km, with many further records from the aftershocks.

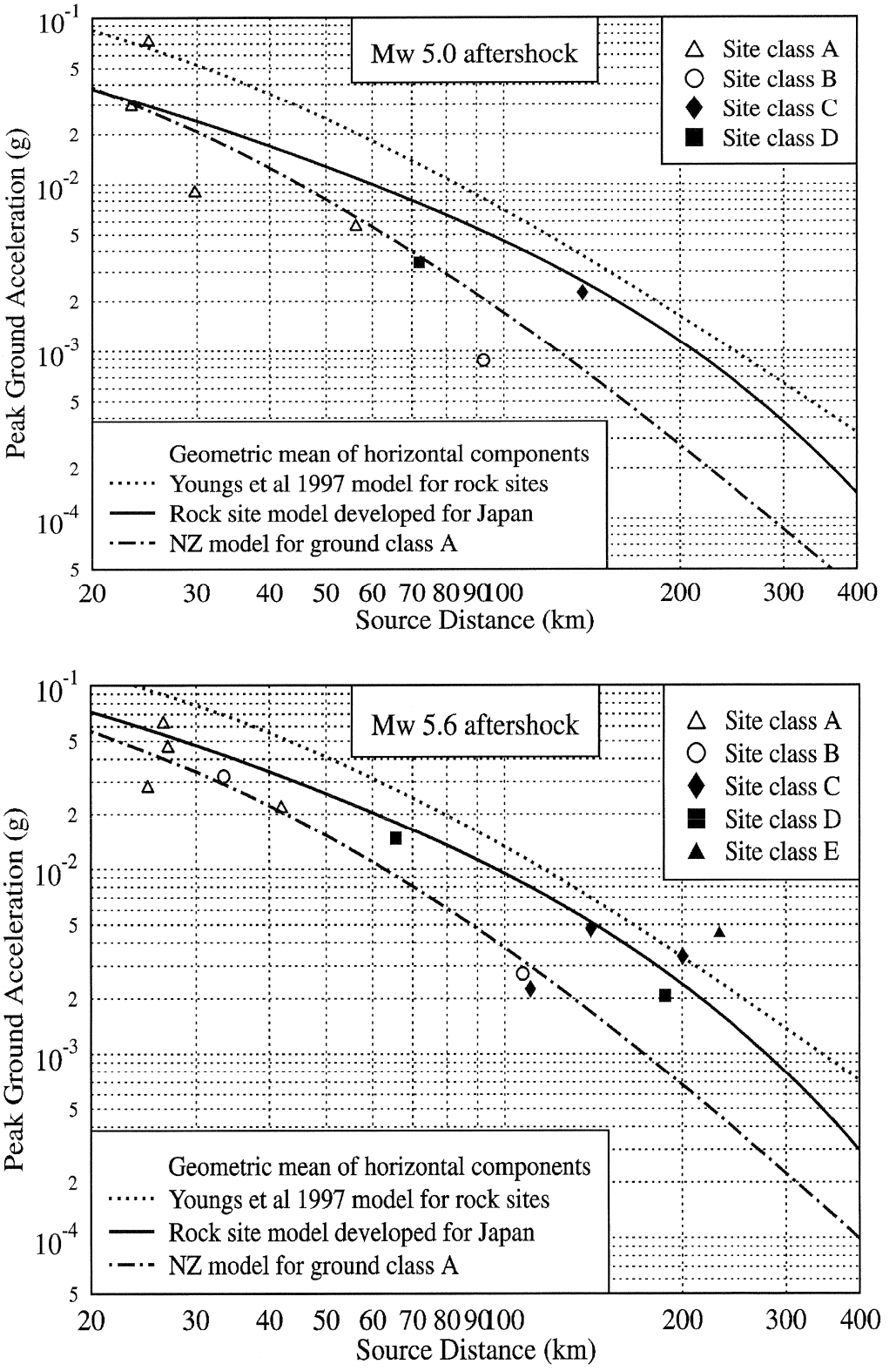

Figure 21: Comparison of the magnitude 5.0 and 5.6 Fiordland aftershock pga data with three attenuation models for rock conditions, appropriate for the data at the shortest distances.

It is not clear whether the discrepancies arise because the nature of the earthquakes and their attenuation are different for Fiordland than for the Hikurangi subduction zone which has provided most of the New Zealand data, or because of deficiencies in the scaling with magnitude. The two previous Fiordland subduction interface earthquakes, and now the 2003 event, are of larger magnitude than any of the other interface earthquakes in the dataset, for which the maximum magnitude was 5.8.

Another issue is that there was a very marked geographical variation in the strength of shaking in the mainshock for a given distance from the source, as discussed in Reyners *et al.* (2003). At this stage, the aftershock data has not been evaluated for any azimuthal dependence, which was such a strong feature in the mainshock data.

These issues are all to be investigated in future work. The nature of the misfits of the data from the Fiordland earthquakes is certainly more complicated than can be handled by scaling estimated spectral accelerations for Fiordland by a period-dependent regional factor.

11. RECOMMENDATIONS FOR THE USE OF THE MODEL

11.1 Magnitude Range

There are several magnitude-dependent features of the model that can lead to overly strong contributions from low- to moderate-magnitude earthquakes in hazard analyses that include events less than about magnitude 5.25.

Two of these features result from the simplification of the linear magnitude term for crustal earthquakes.

First, dropping the Abrahamson & Silva small-magnitude coefficient to better fit the New Zealand data has resulted in a model that produces lower near-source estimates at larger magnitudes than several other models (e.g. Sadigh *et al.*, 1997; Abrahamson & Silva, 1997; Boore, Joyner & Fumal, 1997). Near-source New Zealand data is required to confirm whether this behaviour is real.

In addition, the lesser magnitude-dependence allows smaller magnitude earthquakes to make relatively greater contributions to hazard estimates. This causes smaller magnitudes to over-dominate the hazard for short spectral periods unless the minimum-magnitude cutoff used in the hazard analysis is selected carefully. Combined with the magnitude-dependent standard deviation that is larger for small magnitudes (see Section 6.6), this leads to uniform hazard spectra that peak at shorter periods than the 50-percentile spectra of the contributing events unless the lower magnitude cutoff in the hazard analysis is taken as about 5.25 or greater. This is larger than the lower magnitude cutoff of 5.0 which has become the standard in Californian hazard analyses, but is the same as used in the Matuschka *et al.* (1985) hazard analysis that underlies the current New Zealand Loadings Standard.

In light of this experience, the decision to retain only the large-magnitude coefficient is likely to be revisited, either by allowing a single coefficient for all magnitudes to be fitted from the regression analysis rather than using the Abrahamson & Silva large-magnitude value, or by returning to an intermediate model obtained during the model development in which the value of the small-magnitude coefficient was different from that of the Abrahamson & Silva model.

11.2 Depth Term

The strong dependence on depth in the subduction zone model requires a constraint on the application of the depth term. The large values of the depth coefficients $C_{20}(T)$ for some periods lead to nonsensical values for the predicted accelerations for depths in excess of about 150 km, the maximum depth in the dataset from which the model was derived. To avoid this problem, it is recommended that earthquakes of depth greater than 150 km not be included in hazard analyses, as their real contributions to hazard for levels of motion of engineering significance are slight. If it is desired to include them, it is recommended that the actual depth be used to determine the distance to the source, but that the $C_{20}(T)\ H_c$ depth term be limited to its value at 150 km depth. Atkinson & Boore (2003) found a similar problem

and made a similar recommendation. For their model, they recommended that the depth term should be limited to its value for 100 km depth, the depth cutoff used in their regression analysis, to avoid prediction of unrealistically high accelerations for earthquakes exceeding 100 km depth. The strength of the depth terms is not a problem when slab earthquakes are included only to a maximum depth of 100 km, as in the New Zealand National Seismic Hazard Model of Stirling *et al.* (2000, 2002). For depths between 100 km and 150 km, the attenuation expression begins to give problems for sites located at short horizontal distances above the source.

Although it has a strong effect, the physical significance of the depth term is unclear. Initially, it was assumed that the depth term represented a source effect, reflecting greater stress drops at depth. However, modelling of the attenuation ("*Q*") structure of the Hikurangi Subduction Zone and the upper mantle landward of it in the vicinity of the Taupo Volcanic Zone (Eberhart-Phillips & Chadwick, 2002) and investigation of its effect on the attenuation of earthquake motions (Eberhart-Phillips & McVerry, 2003) shows that the average attenuation per unit path length for subduction earthquakes with propagation paths up the slab (i.e. those not strongly affected by high attenuation in the mantle) is less for deeper earthquakes. Similar behaviour was found by Molas & Yamazaki (1995) for Japanese subduction slab earthquakes.

It seems possible that the depth term is trying to mimic the effects of a depth-varying attenuation rate. At least in part, it appears that the depth-dependent term compensates for an over-estimation of the attenuation of motions from deep earthquakes that occurs when using a constant attenuation rate for all depths. Molas & Yamazaki arrived at a similar conclusion: "Deep events propagate in high-Q zones resulting in lower attenuation rates. In such a case, the larger levels of peak amplitude can be explained by the lower attenuation rate, and the depth term can be regarded as a correction factor to the attenuation rate."

11.3 Volcanic Zone Attenuation

Attenuation in the TVZ is so much greater than elsewhere that it is important to include its effects. Currently, the greater attenuation rate in the TVZ is applied approximately in the NSHM. The TVZ attenuation rate is applied to the total path length for earthquake sources within the TVZ, while not applied for earthquakes originating outside the TVZ. This leads to an under-estimation of the contributions of TVZ sources to the hazard at locations outside the TVZ, as their motions are over-attenuated by applying TVZ attenuation rates to the whole path length, rather than just to that part of it inside the TVZ. On the other hand, contributions from sources outside the TVZ are over-estimated within the TVZ, because the higher attenuation is not applied for that part of the path within the TVZ. In practice, these errors are fairly minor, as generally most of the contribution to the hazard comes from the sources closest to the site, for which the attenuation model is applied correctly. Using TVZ attenuation for TVZ sources has a large effect on hazard estimates within the TVZ, and the approximate procedure is better than ignoring TVZ attenuation completely.

11.4 Mantle Wedge Attenuation

The effects of mantle wedge attenuation are not included in the attenuation model as presented here, and mantle wedge attenuation is not accounted for in maps generated by the NSHM. Implementation of appropriate attenuation expressions for mantle-wedge paths is difficult in hazard maps, as the expressions vary for different source-station pairs, or at least for groups of source-station pairs. Modelling of mantle-wedge attenuation effects has been implemented in some customised hazard studies for a few sites, but not generally. As a first approximation, deep slab sources make little contribution to the hazard at locations involving mantle-wedge paths, so excluding deep slab sources completely for sites overlying the high-loss mantle wedge often provides more realistic results than including them with the standard deep-slab attenuation expression, which is valid only for low-loss propagation paths up the subducting slab. This is particularly true for deep earthquakes for which the estimated motions may be unrealistically large because of the effect of the depth term, as discussed in Section 11.2.

11.5 Behaviour of site class factors with spectral period

As noted at the end of Section 8, an unusual feature of the model is that shallow soil and rock spectra are almost identical at long spectral periods, of 1.5s and greater. This feature is likely to be spurious.

11.6 Smoothing of estimated spectra

To obtain design spectra, the hazard spectra that result from using the New Zealand response spectrum attenuation model presented in this paper often require smoothing, especially for rock and deep or soft soil spectra, for which there are fewer underpinning data than for shallow soil spectra. Often this can be achieved by applying a rising branch proportional to spectral period T from the pga value at zero period to a plateau that approximates the peak of the spectrum, followed by a series of straight-line branches over various period ranges in plots of $lnSA(T)$ versus lnT, i.e. $SA(T)$ proportional to $(T)^{-\gamma}$, with different values of γ in different period bands. Typical values of γ used in various branches for developing design spectra are ⅔ or ¾, 1 (constant spectral velocity) and 2 (constant spectral displacement). The smoothed spectra may be selected to either envelope or lie through the raw hazard estimates, depending on the degree of conservatism required in the recommended spectra.

12. CONCLUSIONS

Attenuation expressions for 5% damped acceleration response spectra and peak ground accelerations have been developed that are appropriate for New Zealand. The expressions have been derived through supplementing local data with near-source world-wide data, and modifying existing attenuation relations to better fit the supplemented New Zealand data. This approach is necessary because New Zealand, like many other regions, has a catalogue of strong-motion earthquake records that is sizeable and sufficient to show differences from earthquake motions recorded elsewhere in the world, but not sufficiently large on its own to develop robust attenuation models.

Particular care has been made to separate earthquakes from different tectonic regimes (crustal, subduction interface and subduction slab) and to account for the high attenuation rates in the Taupo Volcanic Zone. The need for different treatment of crustal and subduction zone earthquakes is most apparent when the effects of source mechanism are taken into account. For crustal earthquakes, reverse mechanism events produce the strongest motions, followed by strike-slip and normal events. For subduction zone events, the reverse mechanism interface events have the lowest motions, at least in the period range up to about 1s, while the slab events, usually with normal mechanisms, generally have the strongest. The relations developed in this study are not appropriate for source-to-site paths from deep earthquakes affected by high attenuation in the mantle above the subducting Pacific Plate in the central North Island.

The site classes are those that have been incorporated into the recently published standard NZS1170.5 for earthquake actions in New Zealand. They have been retained as close as possible to those of the previous standard NZS4203:1992, but this study demonstrated that some changes were desirable. Statistical analysis showed that it was appropriate to define a new shallow soil site class by combining the intermediate soil site class of NZS4203 with those sites with more than 3m of stiff to very stiff soil that are combined with rock sites in NZS4203. The differences between spectra from shallow soil sites and rock sites were found to be statistically significant, with the addition of site-terms to account for these effects being justified by the Akaike Information Criterion. These results are in agreement with recent studies of US datasets (Rodríguez-Marek *et al.*, 2001), but the differences in spectra between rock and shallow soil sites are not accounted for in several current western US attenuation relations that combine rock sites and shallow soil sites up to about 20m depth in a single site category. Weaker spectra are found for rock sites in our study compared to some western US models. The differences may result largely from the rock spectra from the US models actually being rock and shallow soil spectra, with the datasets dominated by shallow soil rather than rock records.

The problems that remain in the models developed for New Zealand are most evident at magnitude and distance

combinations for which data are lacking. Large-magnitude data for subduction zone earthquakes and large-magnitude, near-source data for crustal earthquakes are still required to improve the reliability of estimates of response spectra and pgas at the large amplitudes of most interest in seismic design. Insufficient data lead to spectra with localised peaks and troughs for many magnitude and distance combinations. Accordingly, it is recommended that smoothing be applied to the raw hazard spectra for many design purposes.

13. ACKNOWLEDGEMENTS

The research reported in this paper was funded by the New Zealand Foundation for Research, Science and Technology under Contract CO5506, and by the former Electricity Corporation of New Zealand Ltd.

The first author gratefully acknowledges the interaction with his GNS and US co-authors in the development of the model reported here. He accepts responsibility for the final model, which evolved over several years through a number of intermediate models. As well as the technical input and advice of Norm Abrahamson and Paul Somerville, Norm contributed software implementing the random-effects methodology without which the task would have been much more onerous.

This study has made use of inputs from many GNS staff, either in the form of tasks performed specifically for the study or in providing pre-existing information. This assistance is gratefully acknowledged. In particular, we thank Jim Cousins for providing processed data, and Nick Perrin for assisting with the classification of sites.

The study has built on compilations of New Zealand strong motion data assembled by a variety of GNS staff over several years. The files listing New Zealand accelerograph and seismograph data were compiled largely by Jim Cousins, with contributions by David Dowrick, John Zhao and Terry Webb. The site classifications were largely assigned by the first author, based on the description of site conditions given by Cousins *et al.* (1996). Nick Perrin and Jim Cousins contributed the site descriptions for the National Seismograph Network and the TVZ Temporary Network. The records themselves were accumulated over a period exceeding thirty years by technicians associated with the New Zealand strong-motion and National Seismograph networks, notably Dick Hefford, David Baguley, Shirley O'Kane, Arnold Heine and Pam Horton.

The attenuation models have been developed in parallel with pga attenuation studies comparing accelerograph and seismograph records by Jim Cousins and John Zhao. Some of their results have been used, especially in defining the extent of the highly-attenuating part of the volcanic region. Terry Webb, Aasha Pancha and Kevin Fenaughty performed the ray-tracing calculations associated with determining the volcanic path term. Donna Eberhart-Phillips and Mark Chadwick developed the Q-model that allowed modelling of mantle-wedge attenuation, with Donna performing the ray-tracing to calculate theoretical source-to-site attenuation using this model.

Jim Cousins, John Zhao and Andrew King are thanked for their helpful in-house reviews.

14. REFERENCES

Abrahamson, N.A. and Shedlock, K.M. (1997). Overview, *Seismological Research Letters*, 68(1): 9-23.

Abrahamson, N.A. and Silva, W.J. (1997). "Empirical response spectral attenuation relations for shallow crustal earthquakes", *Seismological Research Letters*, 68(1): 94-127.

Abrahamson, N.A. and Youngs, R.R. (1992). "A stable algorithm for regression analyses using the random effects model", *Bulletin of the Seismological Society of America*, 82: 505-510.

Akaike, H. (1974). "A new look at the statistical model identification", *IEEE Trans. Auto. Control*, AC-19(6): 716-723.

Atkinson, G.M. and Boore, D.M. (2003). "Empirical ground-motion relations for subduction-zone earthquakes and their application to Cascadia and other regions", *Bulletin*

of the Seismological Society of America, 93(4): 1703-1729.

Berrill, J.B. (1985). "Distribution of scatter in New Zealand accelerograph data", *Bulletin of the New Zealand National Society for Earthquake Engineering* 18(2): 151-164.

Bolt, B.A. and Abrahamson, N.A. (1982). "New attenuation relations for peak and expected accelerations of strong ground motion", *Bulletin of the Seismological Society of America*, 72(6): 2307-2321.

Boore, D.M., Joyner, W.B., and Fumal, T.E. (1997). "Equations for estimating horizontal response spectra and peak accelerations from western North American earthquakes: a summary of recent work", *Seismological Research Letters*, 68(1): 128-153.

Brillinger, D.R. and Preisler, H.K. (1984). "An exploratory analysis of the Joyner-Boore attenuation data", *Bulletin of the Seismological Society of America*, 74: 1441-1450.

Brillinger, D.R. and Preisler, H.K. (1985). "Further analysis of the Joyner-Boore attenuation data", *Bulletin of the Seismological Society of America*, 75: 611-614.

Campbell, K.W. (1981). "Near-source attenuation of peak horizontal acceleration", *Bulletin of the Seismological Society of America*, 71: 2039-2070.

Campbell, K.W. (1997). "Empirical near-source attenuation relationships for horizontal and vertical components of peak gropund acceleration, peak ground velocity, and pseudo-absolute acceleration response spectra", *Seismological Research Letters*, 68(1): 154-179.

Cousins, W.J. (1993). "Highlights of 30 years of strong-motion recording in New Zealand", *Bulletin of the New Zealand National Society for Earthquake Engineering* 26(4): 375-389.

Cousins, W.J., Zhao, J.X. and Perrin, N.D. (1999). "A model for the attenuation of peak ground acceleration in New Zealand earthquakes based on seismograph and accelerograph data", *Bulletin of the New Zealand Society for Earthquake Engineering*, 32(4): 193-220.

Crouse, C.B., Vyas, Y.K., and Schell, B.A. (1988). "Ground motions from subduction-zone earthquakes", *Bulletin of the Seismological Society of America*, 78(1): 1-25.

Crouse, C.B. (1991). "Ground-motion attenuation equations for earthquakes on the Cascadia subduction zone", *Earthquake Spectra*, 7(2): 201-236.

Downes, G.L. (1995). "Atlas of isoseismal maps of New Zealand earthquakes, Institute of Geological and Nuclear Sciences", *Monograph 11*.

Dowrick, D.J. and Rhoades, D.A. (1998). "Magnitudes of New Zealand earthquakes". *Bulletin of the New Zealand Society for Earthquake Engineering*, 31(4): 260-280.

Dowrick, D.J. and Rhoades, D.A. (1999). "Attenuation of Modified Mercalli intensity in New Zealand earthquakes", *Bulletin of the New Zealand Society for Earthquake Engineering*, 32(2): 55-89.

Dziewonski, A.M., Friedman, A., Giardini, D. and Woodhouse, J.H. (1983). "Global seismicity of 1982: centroid-moment tensor solutions for 308 earthquakes". *Physics of Earth and Planetary Interiors*, 33:76-90.

Eberhart-Phillips, D. and Chadwick, M. (2002). "Three-dimensional attenuation model of the shallow Hikurangi subduction zone in the Raukumara Peninsula, New Zealand", *Journal of Geophysical Research, 107*, ESE3-1-15.

Eberhart-Phillips, D. and McVerry, G. (2003). "Estimating slab earthquake response spectra from a 3-D Q model", *Bulletin of the Seismological Society of America*, 93(6): 2649-63.

Fukushima, Y., and Tanaka, T. (1990). "A new attenuation relation for peak horizontal acceleration of strong earthquake ground motion in Japan", *Bulletin Seism. Soc. of America*, 80: 757-783.

Haines, A.J. (1981). "A local magnitude scale for New Zealand earthquakes", *Bulletin of the Seismological Society of America*, 71: 275–294.

Idriss I. M. (1991). *Selection of earthquake ground motions at rock sites*, Report prepared for the Structures Division, Building and Fire Research Laboratory, National Institute of Standards and Technology, Department of Civil Engineering, University of California, Davis.

Joyner, W.B. and Boore, D.M. Boore (1981). "Peak horizontal acceleration and velocity from strong-motion records including records from the 1979 Imperial Valley, California, earthquake", *Bulletin of the Seismological Society of America*, 71: 2011-2038.

Katayama, T. (1982). "An engineering prediction model of acceleration response spectra and its application to seismic mapping", *Journal of Earthquake Engineering and Structural Dynamics*, 10: 149-163.

Kobayashi, S., Takahashi, T., Matsuzaki, S., Mori, M., Fukushima, Y., Zhao, J.X. and Somerville, P.G. (2000). "A spectral attenuation model for Japan using digital strong motion records of JMA87 type". *Paper No. 2786, Proceedings 12th World Conference on Earthquake Engineering*, Auckland, New Zealand.

McVerry, G.H. (1986). "Uncertainties in attenuation relations for New Zealand seismic hazard analysis", *Bulletin of the New Zealand National Society for Earthquake Engineering* 19(1): 28-39.

McVerry, G.H., Hodder, S.B., Hefford, R.T. and Heine, A.J. (1984). "Records of engineering significance from the New Zealand strong-motion network", Proceedings of the Eighth World Conference on Earthquake Engineering, San Francisco, California, USA, Volume II, pp.199-206.

McVerry, G.H., Zhao, J.X., Abrahamson, N.A., Somerville, P.G. and Dowrick, D.J. (1998). "New Zealand attenuation relations for crustal and subduction zone earthquakes", *Asia-Pacific Workshop on Seismic Design and Retrofit of Structures*, National Center for Research on Earthquake Engineering, Chinese Taipei.

McVerry, G.H., Zhao, J.X., Abrahamson, N.A. and Somerville, G.H. (2000). "Crustal and subduction zone attenuation relations for New Zealand earthquakes". *Paper No. 1834, Proceedings 12th World Conference on Earthquake Engineering*, Auckland, New Zealand.

Matuschka, T., Berryman, K.R., O'Leary, A.J., McVerry, G.H., Mulholland, W.M, and Skinner, R.I. (1985). "New Zealand seismic hazard analysis". *Bulletin of the New Zealand National Society for Earthquake Engineering* 18: 313-322.

Molas, G.L., and Yamazaki, F. (1995). "Attenuation of earthquake ground motion in Japan including deep focus events", *Bulletin of the Seismological Society of America*, 85: 1343-1358.

Mooney, H.M. (1970). "Upper mantle inhomogeneity beneath New Zealand: seismic evidence", *Journal of Geophysical Research*, 75(2): 285-309.

Mulholland, W.M. (1982). "Estimation of design earthquake motions for New Zealand", *Department of Civil Engineering Report 82-9*, University of Canterbury, Christchurch, New Zealand, 97p.

Mulholland, W.M. (1983). "Estimation of design earthquake motions for New Zealand", *Proceedings of the Third South Pacific Regional Conference on Earthquake Engineering*, Vol. 1, pp. 20-35, Auckland, New Zealand.

NEHRP (National Earthquake Hazard Reduction Program) (1994). *1994 Recommended Provisions for Seismic Regulations of New Buildings: Part 1, Provisions*, Federal Emergency Management Agency, FEMA 222A.

New Zealand Geomechanics Society (1988). *Guidelines for the Field Description of Soils and Rocks in Engineering Use.*

Otsuka, H., Iwasaki, H. and Isoyama, R. (1993). "Attenuation characteristics of near-source motions", *Proceedings International Workshop on Strong Motion Data*, Menlo Park, USA, Vol. 2, 83-98.

Reyners, M., McGinty, P., Cox, S., Turnbull, I., O'Neill, T., Gledhill, K., Hancox, G., Beavan, J., Matheson, D., McVerry, G., Cousins, J., Zhao, J., Cowan, H., Caldwell, G., Bennie, S. and the Geonet team. (2003). "The M_W 7.2 Fiordland earthquake of August 21, 2003: background and preliminary results", *Bulletin of the New Zealand Society for Earthquake Engineering* 36(4): 233-248.

Rodríguez-Marek, A., Bray, J.D. and Abrahamson, N.A. (2001). "An empirical geotechnical seismic site response procedure", *Earthquake Spectra* 17(1): 65-87.

Sadigh, K. Chang, C.-Y., Egan, J.A., Makdisi, F. and Youngs, R.R. (1997). "Attenuation relationships for shallow crustal earthquakes based on Californian strong-motion data". *Seismological Research Letters*, 68(1): 180-189.

Saiki, T., H. Okada, T. Takahashi, K. Irikura, J..X. Zhao, J. Zhang, H.K. Thio, P.G. Somerville, Y. Fukushima and Y. Fukushima. (2003). "Attenuation models for response spectra derived from Japanese strong-motion records accounting for tectonic source types", *13th*

World Conference on Earthquake Engineering. Vancouver, Canada.

Smith, W.D. (1978). "Spatial distribution of felt intensities for New Zealand earthquakes", *New Zealand Journal Geology and Geophysics*, 21: 293-311.

Somerville, P.G. (2000). "Seismic hazard evaluation". *Paper No. 2833, Proceedings 12th World Conference on Earthquake Engineering*, Auckland, New Zealand.

Also reprinted in Special Issue on the 12th World Conference on Earthquake Engineering, Auckland, January-February 2000, *Bulletin of the New Zealand Society for Earthquake Engineering*, 33(3):371-387.

Somerville, P.G., Smith, N.F., Graves, R.W., and Abrahamson, N.A. (1997). "Modification of empirical strong ground motion attenuation relations to include the amplitude and duration effects of rupture directivity", *Seismological Research Letters,* 68(1): 199-222.

Spudich, P., Fletcher, J., Hellweg, M., Boatwright, J., Sullivan, C., Joyner, W., Hanks, T., Boore, D., McGarr, A., Baker, L. and Lindh, A. (1996). "Earthquake ground motions in extensional tectonic regimes", *U.S. Geological Survey Open File Report* 96-292, 352 p.

Spudich, P., Joyner, W.B., Lindh, A.G., Boore, D.M., Margaris, B.M. and Fletcher, J.B. (1999). "SEA99: A revised ground motion prediction relation for use in extensional tectonic regimes", *Bulletin of the Seismological Society of America*, 89(5): 1156-1170.

Standards Australia/Standards New Zealand (2002). *Structural Design Actions– Part 4 Earthquake Actions. Post Public Comment Draft 2 for Sub-Committee Approval.* Draft Joint Australia/New Zealand Standard Draft Number DR 1170.4/PPC2

Standards New Zealand (1992). *NZS4203:1992 Loadings Standard. Code of practice for general structural design and design loadings for buildings.*

Stirling, M.W. (2000). "A new probabilistic seismic hazard model for New Zealand", *Proceedings 12th World Conference on Earthquake Engineering*, Paper 2362, Auckland, New Zealand.

Stirling, M., McVerry, G., Berryman, K., McGinty, P., Villamor, P., Van Dissen, R., Dowrick, D. and Cousins, J. (2000). "Probabilistic seismic hazard assessment of New Zealand". *Client Report 1999/53*, prepared for Earthquake Commission Research Foundation, Institute of Geological and Nuclear Sciences Ltd, Lower Hutt, New Zealand.

Stirling, M.W., McVerry, G.H. and Berryman, K.R. (2002). "A new seismic hazard model for New Zealand", *Bulletin of the Seismological Society of America*, 92(5):1878-1903.

Webb, T.H. and Anderson, H. (1998). "Focal mechanisms of large earthquakes in the North Island of New Zealand: slip partitioning at an oblique active margin", *Geophysical Journal International*, 134: 40-86.

Wilson, C.J.N., Houghton, B.F., McWilliams, M.O., Lanphere, M.A., Weavder, S.D. and Briggs, R.M. (1995). "Volcanic and structural evolution of Taupo Volcanic Zone, New Zealand: a review", *Journal of Volcanology & Geothermal Research*, 68: 1-28.

Youngs, R.R., Day, S.M. and Stevens, J.P. (1988). "Near-field motions on rock for large subduction zone earthquakes", in *Earthquake Engineering and Soil Dynamics II – Recent Advances in Ground Motion Evaluation*, ASCE Geotechnical Special Publication 20, 445-462.

Youngs, R.R., Chiou, S.-J., Silva, W.J. and Humphrey J.R. (1997). "Strong ground motion attenuation relationships for subduction zone earthquakes". *Seismological Research Letters*, 68(1): 58-73.

Zhao, J.X., Dowrick, D.J., and McVerry, G.H. (1997). "Attenuation of peak ground accelerations in New Zealand earthquakes", *Bulletin of the New Zealand National Society for Earthquake Engineering*, 30(2): 133-158.

APPENDIX: STATISTICAL CONSIDERATIONS

Log-likelihood LL of a random-effects model

In terms of the random-effects model, if response spectrum accelerations are assumed to have a log-normal distribution, observation y_{ij} of the logarithm of the jth record of the response spectrum acceleration $SA_{ij}(T)$ for period T in earthquake i can be expressed as

$$y_{ij} = \ln SA_{ij}(T) = g(e_i, s_{ij}, \underline{\beta}) + \eta_i + \varepsilon_{ij} \quad \text{(A1a)}$$

$$= g_{ij} + \eta_i + \varepsilon_{ij} \quad \text{(A1b)}$$

where e_i are variables that are functions of earthquake i (e.g. magnitude, tectonic setting and focal mechanism), s_{ij} are variables for site j in earthquake i (e.g. distance of site j from the source of earthquake i, site conditions at j), $\underline{\beta}$ are parameters of the attenuation model, η_i is the inter-event error for earthquake i and ε_{ij} is the intra-event error at site j in earthquake i. The errors η_i and ε_{ij} are assumed to be independent normal variables with zero means and standard deviations τ and σ_i respectively, where the standard deviation of the intra-event error may be dependent on parameters of earthquake i, such as its magnitude.

The likelihood of the observations y_{ij} across all sites j in earthquake i, $f_i(\underline{y}_i)$, where $\underline{y}_i = (y_{i1}, y_{i2}, \ldots)$, is given by

$$f(\underline{y}_i) = \int_{-\infty}^{\infty} \frac{1}{\sqrt{2\pi}} \exp(-z^2/2) \prod_j \{\frac{1}{\sqrt{2\pi}} \frac{1}{\sigma} \exp[-(y_{ij} - g_{ij} - \tau z)^2 / 2\sigma^2]\} dz \quad \text{(A2)}$$

The likelihood of the complete set of observations y_{ij} in all earthquakes is the product of the likelihoods for the individual earthquakes

$$Likelihood = \prod_{i=1}^{Neq} f_i(\underline{y}_i) \quad \text{(A3)}$$

Finally, the log-likelihood LL of the observations is given by

$$LL = \sum_i \ln f_i(\underline{y}_i) \quad \text{(A4)}$$

Criteria for inclusion or excluding terms in the model

One of the aims of the analysis was to develop a model with the minimum number of terms to satisfactorily represent the data. Eliminating a term worsens the measure-of-fit, i.e. reduces the LL value, and also in general increases the standard deviation of the error, $\sigma_{TOT}(T)$. However, if the change in the measure-of-fit is small, statistical criteria may suggest that the model is in fact a better representation of the data than the model with a slightly improved measure-of-fit but more parameters. As we were seeking to reduce the number of parameters, it was necessary to have criteria available for assessing when reducing the number of parameters represented an improvement in the model despite a decreased measure-of-fit (LL value).

Our analyses provided three types of information that provided guidance as to the acceptability of various forms of the model, and allowed a quantitative measure of the goodness-of-fit of a model that took into account the number of fitted coefficients that it contained.

(i) Normalised covariance

First, the analyses provided the normalised covariance matrix of the estimates for all the coefficients that were free in the regression analysis. The normalised covariance matrix is given by

$$C_{ij\ normalised} = C_{ij} / (C_{ii}\ C_{jj})^{1/2} \quad \text{(A5)}$$

where C_{ij} is the covariance of the estimates of coefficients i and j, and C_{ii} and C_{jj} are the variances for the estimates of coefficients i and j respectively. The value of $C_{ij\ normalised}$ lies between ±1. A value close to zero means that the estimates of

coefficients i and j are largely uncoupled, while $|C_{ij\ normalised}|$ close to 1.0 indicates that the estimates of coefficients i and j are closely coupled. When estimates of two coefficients are closely coupled, a change in the value of one coefficient can be accompanied by a compensating change in the value of the other coefficient so that the measure-of-fit is little affected. Inspection of the normalised covariance matrix to identify values with modulus close to 1.0 indicated coefficients whose estimates were closely coupled, providing candidate pairs for which one parameter could be either constrained or eliminated from the model and the other fitted from the data with little change in the measure-of-fit.

(ii) t-test

A second piece of information provided by the analyses was the estimated standard error S_i for the estimates of all "free" coefficients. It can be shown that the estimates $\hat{C}_i$ of the regression coefficients found from n data points are normally distributed about their "true" values C_i. This property leads to the "t- test" for the ratio $(\hat{C}_i - C_i)/S_i$ to determine the γ confidence level for the "true" value of C_i :

$$-t \leq \frac{\hat{C}_i - C_i}{S_i} \leq t \qquad \text{(A6)}$$

where t is the solution of

$$F(t) = \tfrac{1}{2}(1 + \gamma) \qquad \text{(A7)}$$

and $F(t)$ is the cumulative distribution function of the Students t-distribution with n-p-1 degrees of freedom, where p is the number of coefficients. When the number of data points n is much greater than the number of coefficients p, the Students t-distribution approximates to the Normal distribution, which is what was used in practice in this study. Similarly, there are tests for the hypothesis that the "true" values of two coefficients are equal, $C_i = C_j$.

Knowing the estimated values and their standard errors, these properties allow the assessment of whether a coefficient value is significantly different from zero, from a constrained value, or from the value of some other associated coefficient. Typically bounds of one or two standard errors are considered around the estimated coefficient values, corresponding to 68% or 95% confidence intervals.

In this study, bounds of two standard errors were found to be poor for discriminating between models in many cases, as often both zero and the default Abrahamson & Silva or Youngs *et al.* values were included in this range. Usually only the one standard error bound was considered in this study. However, few decisions to eliminate parameters or free them from their default values were based on the standard error bounds, with the the Akaike Information Criterion (see below) usually being used as the discriminant for eliminating parameters.

(iii) Akaike information criterion (AIC)

The third piece of information that was used in reducing the number of parameters was the log-likelihood value, LL, of the fit. The criterion for the regression analyses was to maximize the likelihood value, or correspondingly the LL value. However, there is a well-known, although somewhat heuristic, criterion for evaluating the quality of fit of models with different numbers of free coefficients P fitted by the regression in terms of their LL values. The Akaike Information Criterion value (AIC) (Akaike, 1974) is defined as:

$$AIC = -2LL + 2P \qquad \text{(A8)}$$

The best fit is deemed to be given by the model that minimizes AIC. This means, reducing the number of coefficients by one gives a better fit if the corresponding reduction in the LL value is less than 1.0. This criterion was found generally to be more "parsimonious" than the one standard error bound in determining which parameters needed to be included in the model i.e. coefficients that had values significantly different from zero according to the one standard error range around the estimated value produced insufficient improvement in the LL value when included in the model to be justified in terms of the AIC.